Pituitary macrophages in homeostasis, development and disease

Henna Lehtonen

Master's thesis

Subject: Biology, Physiology and Genetics
Author(s): Henna Lehtonen
Title: Pituitary macrophages in homeostasis, development and disease
Supervisor(s): Heli Jokela, Tiina Henttinen
Number of pages: 56 pages + supplements 5 pages
Date: 17.3.2022

Tissue-resident macrophages are the major contributors to tissue homeostasis, development and function. Macrophages populate tissues already during embryonic development forming unique pools in tissues. These distinct pools are involved in the development and function of the endocrine system. The pituitary gland is a major endocrine gland regulating the hormone secretion from peripheral target tissues maintaining the body's overall homeostasis. The composition of macrophages or their contribution to the function or development of the pituitary gland is not known. Despite of the crucial roles of macrophages in tissue homeostasis and function, macrophages involve in tumorigenesis. The tumor microenvironment induces changes in macrophage phenotypes converting them to harmful phenotypes, tumor associated macrophages. Tumor associated macrophages contribute to angiogenesis, invasiveness of cancer cells and tumor growth. The functionality of pituitary macrophages in adenomas is not known.

In this thesis, the aim was to resolve the origin of pituitary macrophages and furthermore to study spatial relationships of macrophages and endocrine cells in the pituitary gland, and shed light on their function in a steady and diseased state in mice. The hypothesis was that the pituitary gland houses macrophages from all three origins, from the yolk sac, fetal liver and bone marrow, in steady state. To resolve the embryonic origins, cell-fate mapping studies were conducted, following the fate of labelled yolk sac-derived macrophages. The macrophage compartments during the postnatal development of mice were studied further. Spatial relationships between the pituitary macrophages and endocrine cell types were studied with, two different staining methods to visualise the gland in 3D with a confocal microscope. The functionality of the pituitary resident macrophages was studied in retinoblastoma deficient mice that develop pituitary adenomas in adult mice.

In this thesis, the origin of pituitary macrophages was resolved. In the mice's prenatal and postnatal pituitary gland, macrophages have originated from the yolk sac and fetal liver. The yolk sac-derived macrophages dominated the immunolandscape in the mouse pituitary gland. During the postnatal development, two distinct macrophage populations were identified. Firstly, embryonic-derived macrophage population was formed when fetal liver-derived macrophages shifted their phenotype. Secondly, bone marrow-derived monocytes infiltrated into the pituitary gland and differentiated into tissue-resident macrophages. However, despite the monocyte infiltration, the embryonic derived macrophage population was the major one in the pituitary gland through the mice development. The spatial relationships of macrophages and endocrine cells remains unsolved. The study of functionality of macrophages in disease suggested that retinoblastoma deficient mice do not develop adenomas at 6 months of age and the study will continue in the future with 9-10 months old mice.

Kudosspesifiset makrofagit osallistuvat kudoksien kehitykseen, elimistön sisäisen tasapainon ylläpitoon ja kudosten toimintaan. Kudosspesifiset makrofagit siirtyvät kudoksiin jo alkionkehityksen aikana ja muodostavat kudoksiin ainutlaatuisia solupopulaatioita, jotka voivat säilyä ja proliferoitua aikuisuuteen asti. Nämä makrofagipopulaatiot osallistuvat umpieritysjärjestelmän kehitykseen ja toimintaan. Aivolisäkkeellä on merkittävä rooli umpieritysjärjestelmässä, jossa se säätelee hormonien eritystä periferisistä umpirauhasista ylläpitäen elimistön tasapainoa. Kudospesifisten makrofagien kokoonpanoa tai populaation osallisuutta aivolisäkkeen toimintaan ja kehitykseen ei ole tutkittu. Vastoin makrofagien kudosten tasapainotilaa ylläpitäviä toimintoja, makrofagit osallistuvat kasvainten muodostumiseen. Syöpäsolujen luoma mikroympäristö kudoksessa indusoi muutoksen makrofagien fenotyypeissä, saaden aikaan haitallisia makrofageja. Haitalliset makrofagit edistävät angiogeneesiä, syöpäsolujen invasiivisuutta ja kasvaimen kasvua. Aivolisäkkeen makrofagien osallisuutta aivolisäkekasvaimissa ei vielä tiedetä.

Tämän tutkielman tavoite oli selvittää hiiren aivolisäkkeen makrofagien alkuperä. Lisäksi tavoitteena oli tutkia aivolisäkkeen makrofagien ja endokriinisolujen spatiaalisia suhteita sekä makrofagien toiminnallisuutta homeostaasissa ja sairaudessa hiirissä. Hypoteesina oli, että aivolisäkkeen makrofagit ovat peräisin kolmesta lähteestä, ruskuaispussista, alkion maksasta ja luuytimestä. Tutkimuksessa selvitettiin leimattujen makrofagien kulkeutumista ruskuaispussista hiiren aivolisäkkeeseen ja miten kudosspesifiset makrofagi populaatiot muuttuvat hiiren yksilönkehityksen aikana.

Makrofagien ja endokriinisolujen välisiä suhteita havainnollistettiin kahdella eri immunohistokemiallisella värjäysmenetelmällä ja konfonkaalikuvantamisella. Makrofagien toiminnallisuutta tutkittiin hiirimallilla, jossa hiirille kehittyy aivolisäkkeen etulohkoon kasvain.

Tässä tutkielmassa todistettiin, että makrofagit ovat läsnä aivolisäkkeessä ennen hiiren syntymää ja hiiren yksilönkehityksen ajan. Alkiossa ja vastasyntyneen hiiren aivolisäkkeessä makrofagien osoitettiin olevan peräisin sekä ruskuaispussista että alkion maksasta. Suurin osa hiiren aivolisäkkeen makrofageista oli peräisin ensimmäisestä populaatiosta eli alkion ruskuaispussista.

Hiiren syntymän jälkeen havaittiin aivolisäkkeessä kaksi eri makrofagipopulaatiota. Ensiksi, alkion maksasta aivolisäkkeeseen kulkeutuneiden makrofagien fenotyyppi muuttui ja aivolisäkkeeseen muodostui yksi populaatio, joka sisälsi sekä ruskuaispussista että alkion maksasta tulleet makrofagit. Toiseksi, luuytimen tuottamat monosyytit kulkeutuivat aivolisäkkeeseen ja erilaistuivat kudosspesifisiksi makrofageiksi, muodostaen toisen populaation.

Hiiren aivolisäkkeen makrofagien ja endokriinisolujen väliseen spatiaalisiin suhteisiin tutkimus ei tuonut lisäinformaatiota. Makrofagien funktionaalisuuden tutkiminen kasvaimen kehityksen aikana viittasi, että tutkimuksessa käytettyihin hiiriin ei kehittynyt kasvainta kuuden kuukauden iässä. Jatkotutkimukset tullaan tekemään vanhemmilla, noin 9—10 kuukauden ikäisillä hiirillä.

Contents

1   Introduction

1.1   Macrophages

Macrophages are cells of mononuclear phagocyte system and key-players of the innate immunity. Along with their inflammatory responses, macrophages have essential non-immunological functions. Macrophages are involved in the development, remodelling and normal function of tissues (Shaw et al. 2018; Utz et al. 2020). In addition, macrophages contribute to the overall homeostasis of the body interacting with the endocrine system (Rehman et al. 2021). Macrophages do not appear as a homogenous population of phagocytic monocytes, rather they show variation in their physiological functions induced by signals of microenvironments where they reside and ontogeny.

Macrophages populate tissues during embryonic development. During embryogenesis embryonic-derived macrophages migrate into tissues from two origins, from the yolk sac and the fetal liver. After birth, tissues can recruit circulating bone marrow-derived monocytes besides macrophages from embryological origins. As a result, macrophages from different origins form heterogeneous pools that remain in tissues and contribute tissue function. These heterogeneous pools of morphologically distinct macrophages are referred to as tissue resident macrophages.

Each tissue has its own composition of embryonically derived and adult bone marrow-derived macrophages. However, it is still unclear whether macrophages of distinct origins have unique roles at steady state or are the roles interchangeable. There is evidence that ontogeny and signals from the tissue microenvironment could shape macrophage function and phenotype (Utz et al. 2020). The research on macrophage ontogeny has challenged the macrophage division to proinflammatory, classically activated macrophages (M1) and anti-inflammatory, alternatively activated macrophages (M2) (Pollard 2009). The division to M1 and M2-macrophages is dichotomous, when recent studies indicate that the activation of macrophages is more multidimensional (Ginhoux et al. 2016; Chanmee et al. 2014). However, despite of the contribution of macrophages in tissue homeostasis and function, it has been shown that macrophages have an effect on different pathological conditions, such as tumorigenesis, neurodegenerative diseases and type 1 diabetes (Chanmee et al. 2014; Geutskens et al. 2005; Utz et al. 2020). Macrophages' anti- and pro-inflammatory roles in human diseases have made them important therapeutic targets.

1.1.1   Origin of tissue-resident macrophages

Tissue-resident macrophages derive from three different origins: yolk sac, fetal liver and bone marrow. Tissues are populated in two waves during embryonic development (Figure 1). In mice, haematopoiesis starts at embryonic day (E) 7 when erythromyeloid progenitors (EMPs) emerge in the blood islands and capillary endothelia of an extra-embryonic structure, the yolk sac (Munro & Hughes 2017). In mice, the first wave derives from the yolk sac, when yolk sac-derived macrophages start to migrate into tissues at E8.5 after embryos vasculature and yolk sac's vasculature connect (Hoeffel & Ginhoux 2018; Munro & Hughes 2017). The yolk sac-derived macrophages populate tissues including the fetal liver at E8.5-E10 (Hoeffel & Ginhoux 2018). The second wave consists of monocytes that derive from the fetal liver. The fetal liver monocyte progenitors are late EMPs derived from the yolk sac and hematopoietic stem cells (HSCs), which are generated by hemogenic endothelium (Munro & Hughes 2017). In mice, the second wave occurs at E12.5 (Hoeffel & Ginhoux 2018). After birth, the bone marrow starts to produce monocytes that migrate in blood circulation and infiltrate into tissues. In tissues, bone marrow-derived monocytes differentiate to macrophages and remain in the tissue. Recent studies indicate that most adult tissues are established by the tissue-resident macrophages during embryonic development and not from circulating monocytes postnatally as previously thought (Jokela et al. 2019; Jäppinen et al. 2018; Ginhoux et al. 2016). Tissue-resident macrophage populations can maintain independently in homeostasis or proliferate as a response to inflammatory state without monocyte recruitment (Jenkins & Allen 2021).
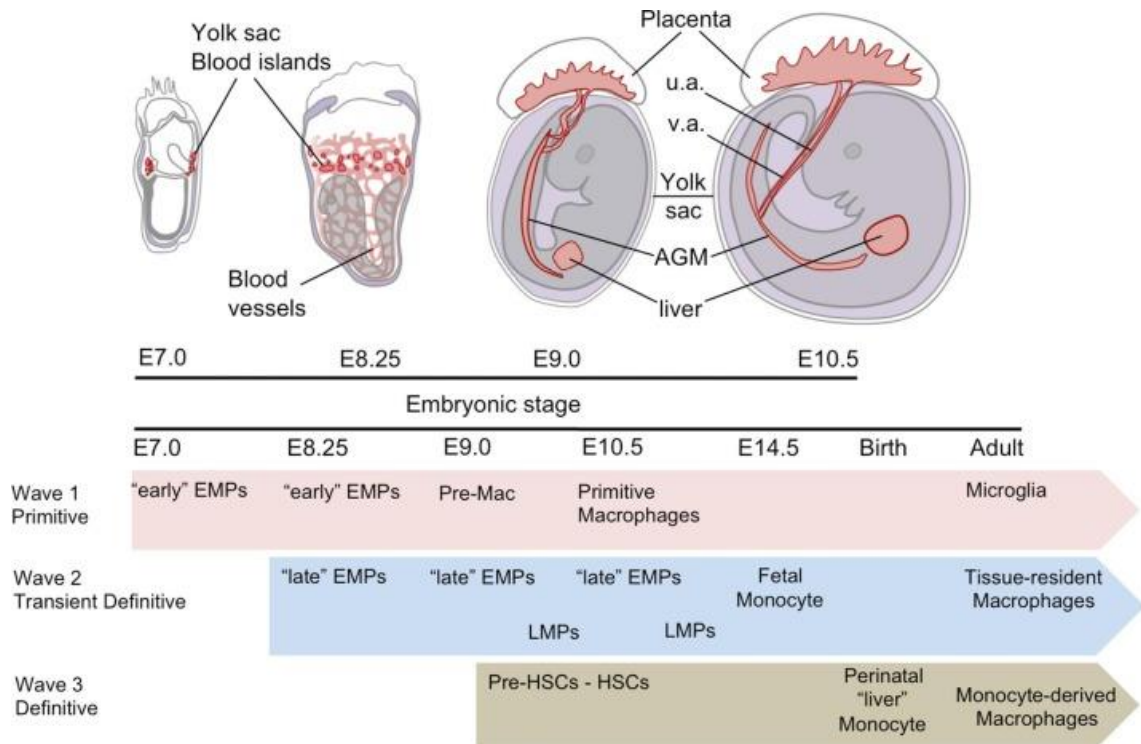
Figure 1. Embryonic hematopoietic programs seeding from the yolk sac and fetal liver during embryonic development in mice. The haematopoiesis starts at E7.0 in the yolk sac blood islands and gives rise to the first wave from the yolk sac at E8.5 of early erythromyeloid progenitors (EMPs) that differentiate to pre-macrophages (Pre-Mac) and primitive macrophages. Transient wave occurs at when late EMPS from the yolk sac migrate into the fetal liver and give rise to fetal monocytes. The hematopoietic stem cells (HSCs) seed from the hemogenic endothelium differentiates to liver monocytes. The second wave generates lymphomyeloid progenitors (LMPs) that provide T and B lymphoid precursors. V.a is vitteline artery and u.a is umbilical artery. Figure: Hoeffel & Ginhoux 2018.

Prenatal macrophages from the embryological origins and the postnatal bone marrow-derived macrophages coexist in many tissues under homeostatic conditions. It has been shown that adipose tissue, gut, mammary gland, spleen and ovary have macrophages from all three origins in tissue-dependent compositions (Félix et al. 2021; Jokela et al. 2020; Jäppinen et al. 2019; Shaw et al. 2018). In the mammary gland, the embryonic-derived macrophage population is the dominant population with the majority consisting of fetal liver-derived macrophages in adult mice (Jäppinen et al. 2019). Also in the testis, fetal liver-derived macrophages are major the contributors in the prenatal and postnatal macrophage pools (Lokka et al. 2020). In the spleen, the composition of macrophages with different origins depends on whether they reside in the red pulp, white pulp or marginal zone (Fujiyama et al. 2018). Spleen resident macrophages express physiological and morphological heterogeneity based on their ontogeny and adaptation to the microenvironment in the spleen (Fujiyama et al. 2018). Also, tissue can house heterogenous macrophage populations with different origins and replenishment rates. Shaw and others (2018) discovered that gut sustaining three different gut-resident macrophage populations recruit monocytes in different levels: independent, moderately renewal and highly replenishment

populations. In homeostasis, gut-resident macrophages was thought to rely on constant recruitment of bone-marrow derived monocytes. Compared to the above mentioned, brain is a unique environment containing only locally maintained yolk sac-derived macrophages without the contribution of fetal liver or bone marrow-derived macrophages in the steady state (Utz et al. 2020).

Tissue-resident macrophages are involved in the development and remodelling of the tissues. Kinetic analyses in mice have shown that macrophage composition change during development altering the relative proportions of the yolk sac, fetal, and bone marrow-derived macrophages. (Utz et al. 2020; Jokela et al. 2020; Hoeffel et al. 2015). In mouse kidneys, dramatic change occurs during between embryonic development and adulthood. The kidney resident macrophage population is established by yolk sac-derived macrophages following fetal macrophages (Hoeffel et al. 2015). In adult mouse, the fetal liver-derived macrophages have exceeded the yolk sac-derived macrophages and dominate in the kidney with low infiltration rate of monocytes (Hoeffel et al. 2015). Similar shift is observed in mice ovaries. In the ovaries, the relative proportion of fetal liver-derived macrophages increases during the embryonic development and in adult, bone marrow-derived monocytes have emerged into the ovaries after birth (Jokela et al. 2020). In heart, yolk sac-derived macrophages establish the pool and persist as a significant proportion in adult mouse in the side of fetal liver-derived macrophages and bone marrow monocytes (Epelman et al. 2014). The discoveries considering the changing composition of the yolk sac and fetal-derived macrophages and different infiltration rates of monocytes suggest that tissue resident macrophage pools are formed during development to generate an unity that contribute to the functions and maintenance of homeostasis in the unique tissue environment.

Cell-fate mapping method with genetically engineered mouse lines is used in the research of origins of tissue-resident macrophages. Fate mapping studies have provided evidences of the origin of macrophages in the tissue of interest, but also proves that embryonic-derived macrophage populations can maintain themselves independently without the recruitment of bone marrow-derived monocytes (Yona et al. 2013). Drug-inducible cre/loxP-reporter mice are very useful studying macrophage ontogeny spatially and temporally. Cre/loxP-utilizing fate mapping models allow labelling of a specific macrophage lineage during embryonic development or at later timepoints, and following up the fate of the labelled cells and their descendants. Cre/loxP-system utilizes site specific recombination of *loxP*-sequence generated by P1 phage Cre-recombinase (Kim et al. 2018). Cre/loxP-system demands crossing of two mouse lines and the labelling is expressed in the offspring. Cre-driver strain that expresses the Cre-recombinase upstream of a promoter in tissue or cells of interest and mouse line that has *loxP*-flanked STOP-sequence in upstream of a marker gene are needed. *loxP*-flanked mice have a construct of STOP-

sequence downstream of a marker gene, for example fluorescent protein coding gene. The STOP-sequence inhibits the reading of the marker gene, and the gene is not expressed in parents. With the crossing of these two mouse lines Cre-recombinase induces site-specific deletion knocking of the STOP-sequence between *loxP*-flanked sequences (Figure 2). As a result of the deletion, the marker gene is functional to code protein in the offspring. To achieve temporally more accurate labelling and induce the signal of fluorescent protein coding genes, drug-inducible Cre/loxP-systems have been developed (Kim et al. 2018). A tamoxifen-inducible Cre-mice created by Metzger and Chambon (2001) have a fusion of mutated ligand domain of estrogen receptor with the Cre-recombinase. This produces tamoxifen-dependent Cre-recombinase construct (CreERT) that able cell/tissue- and time-specific induction of the marker gene (Metzger & Chambon, 2001). Fate mapping studies have shown that microglia are derived from embryonic precursors from the yolk sac (Utz et al. 2020).
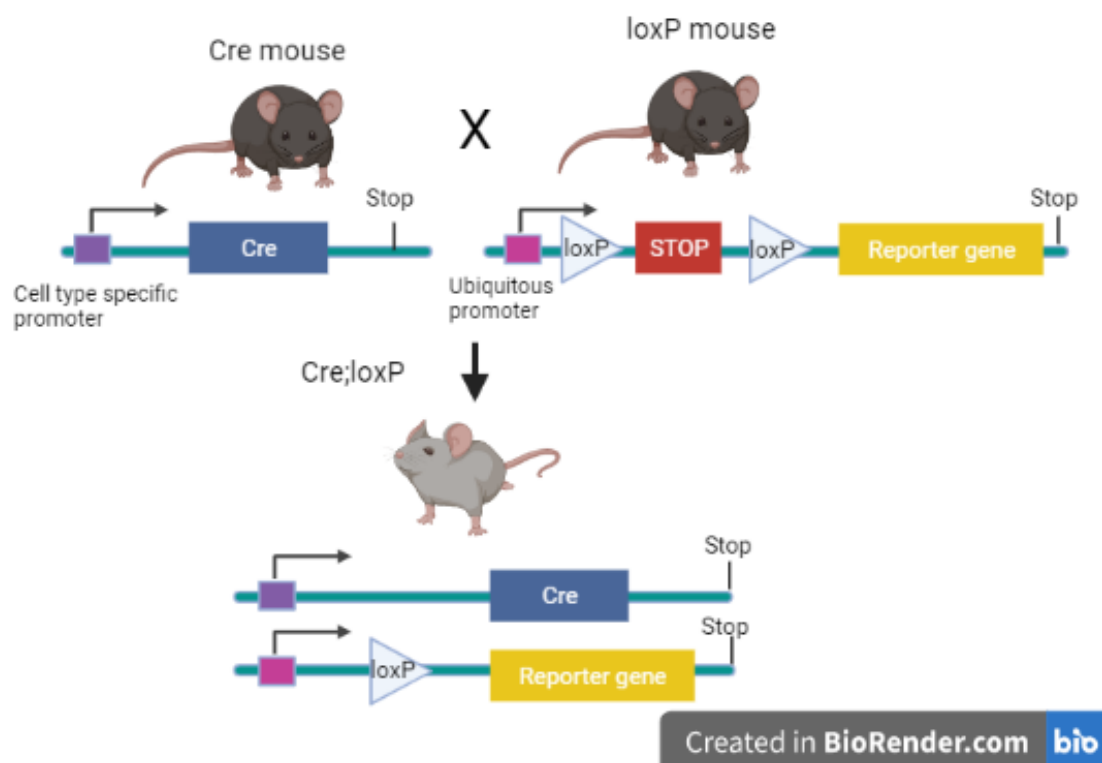
Figure 2. A schematic representation of the Cre/loxP-system in a crossing of Cre and loxP-expressing mice lines. Cre-recombinase induces site-specific deletion knocking of the STOP-sequence between the loxP-flanked sequences in the offspring of the Cre;loxP crossing. In the offspring the reporter gene is translated into a protein in cells that express the chosen cell type specific promoter.

Macrophages can be then labelled with tamoxifen at specific time and followed during life cycle of a mouse. To determine the fate of the yolk sac derived macrophages, the induction of the labelling drug is administered before the fetal liver starts the haematopoiesis. Labelling at E9.5, will induce the fluorescent in a reporter crossing. The descendants of the yolk sac-derived macrophages have the label through the proliferation of these cells. The further division of

macrophages based on their origin can be done based on the cell surface-marker expression at different time points. Surface-marker expression combined with tamoxifen labelling allows tracking cells with site- and time-specific manner.

1.1.2   Identification of macrophages with macrophage markers

Tissue-resident macrophage populations are heterogenic, and their function is versatile to environmental stimulus. During development macrophages are activated by transcription factors, cytokines and most importantly, signals from tissue-generated microenvironments (Ginhoux et al. 2016; Pollard 2009). Responses to external signals are essential for macrophage activation and maintenance of tissue homeostasis. Ontogeny, time spent in the tissue and inflammatory status have been shown to model tissue-specific phenotypes (Blériot et al. 2020; Utz et al. 2020). Tissue-resident macrophages show plasticity and tissue can house multiple subpopulations.

Macrophages can be distinguished from other leukocytes and further identified to distinct tissue-resident macrophage populations by their expression of differential profiles of cell-surface markers. Generally, cells of mouse mononuclear phagocyte system are identified by the expression of antigen receptors including CD45, CD11b, F4/80, Ly6C and CX3C chemokine receptor 1 (CX3CR1). CD11b and F4/80 are the major macrophage markers that are used to specify tissue-resident macrophages and investigate the origins (Ginhoux & Guilliams 2016; Valor et al. 2015). CD45 antigen is expressed in all hematopoietic cells. During the embryonic development the colonisation of tissues is CX3CR1 dependent and macrophages can be characterized from monocytes based on their CX3CR1 expression in prenatal mice (Mass 2018). In adult mice, CX3CR1 is widely expressed in immune cells. Embryonic-derived macrophages can be distinguished from bone marrow-derived monocytes based on their negative Ly6C-expression (Yang et al. 2019).

In order to characterise tissue-resident macrophage populations, other immune cell markers such as mannose receptor CD206 and T-cell membrane protein 4 (TIM-4) should be combined with CD11b and F4/80 expression. As an example, TIM-4 and CD4 expression can used to identify small intestine resident macrophages and TIM-4 and CD163 markers are suitable for characterisation of adipose tissue macrophages (Félix et al. 2021; Shaw et al. 2018). Epelman and colleagues (2014) were able to identify four cardiac macrophage subsets in the mouse heart by first characterising tissue-resident macrophages as CD45+CD11b+F4/80+ and then investigating with further macrophage markers, such as CX3CR1 and CD206, also taking advantage autofluorescence of the cells. In other hand, CD11b and F4/80 are used to identify embryological

origins of tissue-resident macrophages. Yolk sac-derived macrophages express CD11b at intermediate level and F4/80 expression is high. In the fetal liver-derived macrophages the situation is the opposite, high CD11b-expression and intermediate F4/80-expression (Utz et al. 2020; Ginhoux & Guilliams 2016; Schulz et al. 2012).

Transcriptional studies can be combined with methods, such as cytometry, which are able to sort out different phenotypes. Flow cytometry stands as one of the most successful analytical tools to characterise macrophage phenotypes. By using the approach of combined single-cell RNA-sequencing (scRNA-seq) and flow cytometric analysis Utz and others (2020) were able to find two distinct brain macrophage populations: microglia and border-associated macrophages (BAMs). BAMs expressed markers, such as CD206, lymphatic endothelial hyaluronic acid receptor 1 (Lyve1) and scavenger receptor CD163 which were not expressed by microglia. In the other hand, microglia were identified by higher CD11b expression (Utz et al. 2020). Combining CD206 expression with CD11b and F4/80 expressions, authors were able to identify BAMs and microglia as distinct brain resident macrophage population that segregate early during brain development (Utz et al. 2020).

Unique tissue microenvironments might induce macrophages to express distinct surface markers though epigenetic and transcriptional regulation. This in turn creates tissue-specific phenotypes, which function properly in the tissue in question. Transcriptional studies have revealed differences in gene regulation between tissue-resident macrophage populations resulting in heterogenous cell-surface structures of macrophage subpopulations (Utz et al. 2020; Liu et al. 2019).

1.2   Pituitary gland

Pituitary gland is the major component of the endocrine system that controls internal body functions, regulates body's responses to changes in the environment and underlies homeostasis. Endocrine system involves multiple peripheral glands and organs forming complex pathways and feedback loops throughout the body. Pituitary gland controls other endocrine tissues by secreting various hormones from specialised hormone-producing cells regulating growth, reproduction, sexual maturation, pregnancy, metabolism, lactation and stress responses. Pituitary hormones can stimulate hormone secretion or have a direct impact on the metabolism of the tissue respectively. Hormones travel to target tissues via blood circulation and bind to specific receptors in target tissues causing physiological responses.

1.2.1 Basic anatomy of pituitary gland

In humans, the pituitary gland, which is approximately size of a pea, locates in the midline of the skull on the sphenoid bone in a hollow called sella turcica below hypothalamus. The pituitary gland is connected to hypothalamus via pituitary stalk referred as infundibulum. In mice, the pituitary gland lies on the dorsal surface of the basiphenoid skull bone in a midline shallow depression (*sella turcica*) connected to hypothalamus. Pituitary gland consists of three lobes: anterior lobe (adenohypophysis), intermediate lobe and posterior lobe (neurohypophysis). During organogenesis, the adenohypophysis and neurohypophysis originate from two developmentally distinct embryological origins leading to physiological differences in hypothalamic signaling and histological differences in cell types. In mice, the anterior lobe surrounds the posterior lobe and between them lies intermediate lobe. Mouse pituitary gland differs from humans' pea-shaped gland forming a planar capsule-shaped structure where adenohypophysis and neurohypophysis are clearly distinguishable.

The adenohypophysis and neurohypophysis develop from different embryological origins. The anterior lobe originates from the oral ectoderm, while the origin of the posterior lobe is the neural ectoderm. During week 4 of fetal, development of pituitary gland begins when oral ectoderm forms a cell thickening, the hypophyseal placode, which gives rise to the Rathke's pouch (Larkin & Ansorge 2017). In mice, organogenesis of pituitary gland initiates at 7.5 days post coitum. Rathke's pouch grows anteriorly from the oral ectoderm towards the neural ectoderm forming a hollow structure. Eventually, the base of Rathke's pouch constricts and separates from the oral ectoderm. Cells in the anterior wall of the structure undergo proliferation and differentiation to form the adenohypophysis and specialized hormone-producing cells in it. The dorsal region of Rathke's pouch gives rise to the intermediate lobe (Zhu et al. 2005). Posterior lobe develops from the floor of the diencephalon (3th ventricle) i.e. the same structure as the hypothalamus and brain. The diencephalon extent ventrally forming the posterior lobe, finally confronting the anterior lobe. The distinct embryological origins of the lobes are noticeable in the histological appearance of the gland in mice (Figure 3). The majority of the adenohypophysis which is epithelial origin consists of specialized hormone-producing cells. The neurohypophysis consists of axons arising from groups of hypothalamic neurons. In humans, the intermediate lobe is located between the adenohypophysis and neurohypophysis. It is rudimentary and reduced in size compared to rodents (Larkin & Ansorge 2017).
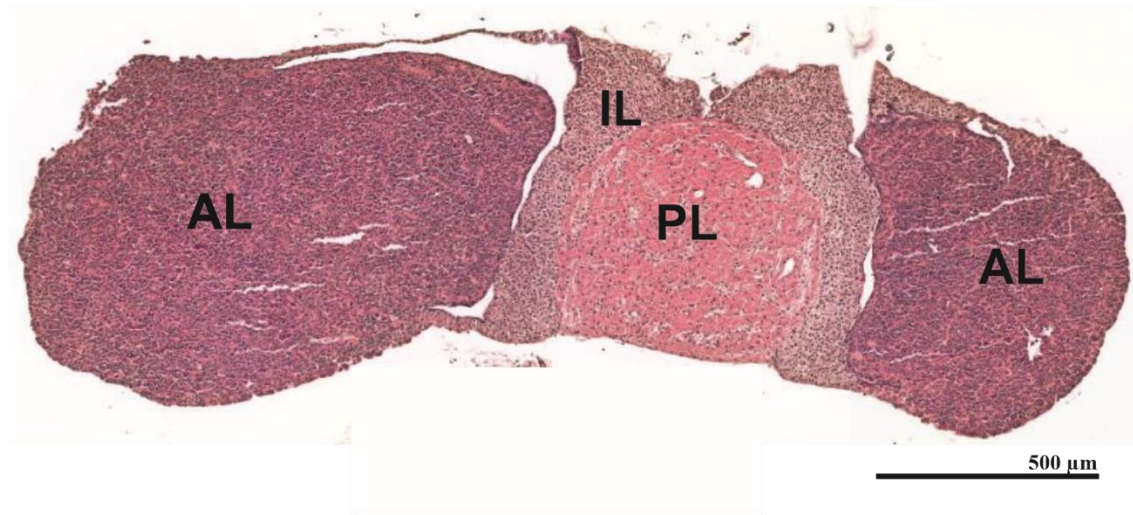
Figure 3. Histological coronal section of a male mouse pituitary gland. Distinct histological appearance of the adenohypophysis (AL), the neurohypophysis (PL) and intermediate lobe (IL) of hematoxylin-eosin stained pituitary gland. The adenohypophysis consisting endocrine tissue stains in deeper colour, when the neurohypophysis consisting neural tissue stains pink. The intermediate lobe surrounds the neurohypophysis.

The adenohypophysis is essential endocrine tissue that sustain five different hormone-producing cell types and non-endocrine cell type, folliculo-stellate cells (FSCs). FSCs have a star-shaped appearance and they reside between endocrine cells involving regulation and maintenance of endocrine cells through interconnections (le Tissier et al. 2012). The five endocrine cell types are specified by the hormone they produce: thyrotropes secrete thyroid-stimulating hormone (TSH), gonadotropes secrete luteinizing hormone (LH) and follicle-stimulating hormone (FSH), corticotropes secrete adenocorticotropic hormone (ACTH) and somatotropes secrete growth hormone (GH) and lactotropes secrete prolactin (PRL).

The neurohypophysis is connected directly to the hypothalamus with neurosecretory magnocellular neurons and does not sustain endocrine cells (Sheng et al. 2021). However, oxytocin (OT) and antidiuretic hormone (ADH) are secreted from the neurohypophysis. OT and ADH are synthesised in the hypothalamus by supra-optic and paraventricular nuclei and then transported via axons to the neurohypophysis (Sheng et al. 2021; Zhu et al. 2005). OT and ADH are then stored in the neurohypophysis and secreted on action potential from the hypothalamus. Also, in the intermediate lobe hormone-producing cell type, melanotrope, is present. Melanotropes secrete melanocyte-stimulating hormone (MSH) from the intermediate lobe. MSH regulates the production and release of melanin from melanocytes.

The endocrine cells show distinct localisation in the adenohypophysis and are not evenly distributed (Larkin & Ansorge 2017; Ooi et al. 2004). Somatotropes are the most common endocrine cell type in the adenohypophysis covering 50% when thyrotropes are the least common

(Ooi et al. 2004). Study of the regionality of endocrine cell types in developing mice, Davis and others (2011) were able to show enrichment areas of the endocrine cell types in embryonic state. They discovered that gonadotropes were located rostral locations and somatotropes were caudally distributed when corticotropes and thyrotropes were enriched more intermediately in the adenohypophysis of developing mice (Davis et al. 2011). During the development, various transcription factors and other regulative elements involve the development and specialisation of endocrine cell types present in the pituitary gland. In mice, endocrine cells show temporal variation in differentiation when most of the endocrine cells are specified between E11.5-E13.5 when lactotropes, as an example, shown to specify after birth (Davis et al. 2011). According to Zhu and others (2005) in humans the differentiation of endocrine cell types is completed during the first trimester, but in mice the specialisation is completed after birth.

The 3D visualisation of the pituitary gland has led to discoveries of the cell organisation. Instead of thin two-dimensional histological sections, 3D has improved the study of the location and distribution of endocrine cells and their spatial relationships with the pituitary vasculature. The endocrine cells were considered to form a random patchwork in the adenohypophysis. The 3D imaging has revealed that endocrine cells are organized into structural and functional networks during organogenesis and show diverse associations to the vascular network (le Tissier et al. 2012; Budry et al. 2011; Davis et al. 2011). The GH-producing somatotropes are found close to blood vessels surrounded by capillaries and connect to each other with adherent junctions forming a network that expands throughout the pituitary (le Tissier et al. 2012; Budry et al. 2011). Corticotropes and gonadotropes form integrated networks, but gonadotropes are closely associated with vasculature whereas corticotrophes show distant localisation (le Tissier et al. 2012; Budry et al. 2011).

The organization of endocrine cells into networks allows rapid signaling and response to external and internal stimulus enhancing the function of the pituitary gland. The pituitary is well-vascularised and the vasculature is organised into network to transport hypophyseal hormones, pituitary hormones and support tissue homeostasis (Figure 4). The pituitary vasculature is connected with the hypothalamus via the hypophyseal portal system. The vasculature branches into capillaries that can surround cell clusters. The blood flow in the gland is locally modified in a response of stimulation to secrete hormones. The secreted products are transported via pituitary vasculature and cleared from the gland to periphery. Also, hormone secretion increases metabolic needs of active endocrine cells. Effective vascular network in the gland is essential for the dynamic regulative function of the pituitary gland.
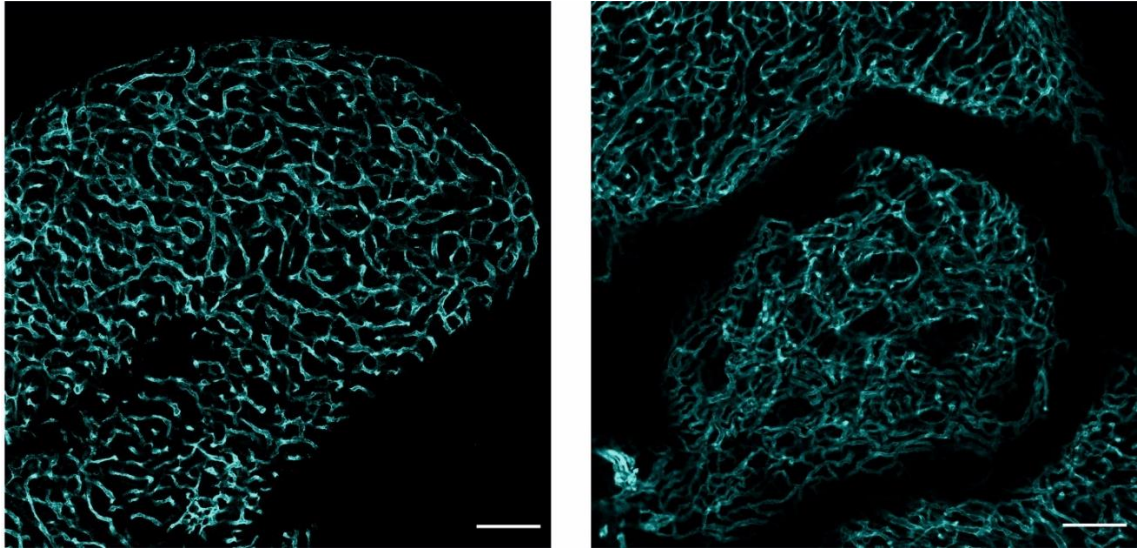
Figure 4. Vasculature of the mouse pituitary gland. Immunohistochemical staining of the pituitary vascular network with panendothelial marker. Staining visualises pituitary vasculature in 8-weeks-old mice adenohypophysis (left) and neurohypophysis (right). Scale bar 100 µm.

1.2.2 Physiology of pituitary gland

The pituitary gland maintains homeostasis of the body as in guidance of the hypothalamus. The regulation of body's state occurs by secreting hormones from the specialised endocrine cells as a response to stimulus. The control of a stable state requires constant monitoring of hormone levels in blood and involves neuroendocrine signaling and signals from peripheral organs. Hormone secretion is decreased or increased from the pituitary as a response to the current state in the body.

Hypothalamus is part of the brain locating on the under of the brain. Based on signals from peripheral organs and brain, hypothalamus inhibits or enhance hormone secretion from the pituitary gland. Hypothalamus signals to the adenohypophysis through hypophyseal portal system with hypophysiotrophic hormones. Hypophyseal portal system is a network of blood vessels between the hypothalamus and adenohypophysis which transport released hormones from the hypothalamus. As opposed to the adenohypophysis, the neurohypophysis is in direct connection to the hypothalamus through nerves running down the pituitary stalk and signaling do not require hypophysiotrophic. Instead, hypothalamus sends signals straight down the magnocellular neurons. Action potential induces hormone exocytosis from the neurohypophysis.

Hypophysiotrophic hormones are produced and secreted by the hypothalamus. There are five major hypophysiotrophic hormones: growth hormone-releasing hormone (GHRH), prolacting releasing hormone (PRH), corticotropin-releasing hormone (CRH), thyroid stimulating hormone (TRH) and gonadotropin-releasing hormone (GnRH). These hormones travel to the pituitary gland and bind to a receptors of a specific endocrine cell type in the adenohypophysis described

before. Binding to the receptor induces or represses hormone production in the gland. The pituitary hormones travel in blood circulation to target glands or tissues regulating secondary hormone production from the target tissue or inducing a function such as growth of bone (Figure 5). The effects of the hormones secreted from the adenohypophysis are trophic or direct. Trophic hormones regulate hormone secretion of other endocrine glands when directly acting hormones have a direct effect on the gland or tissue.
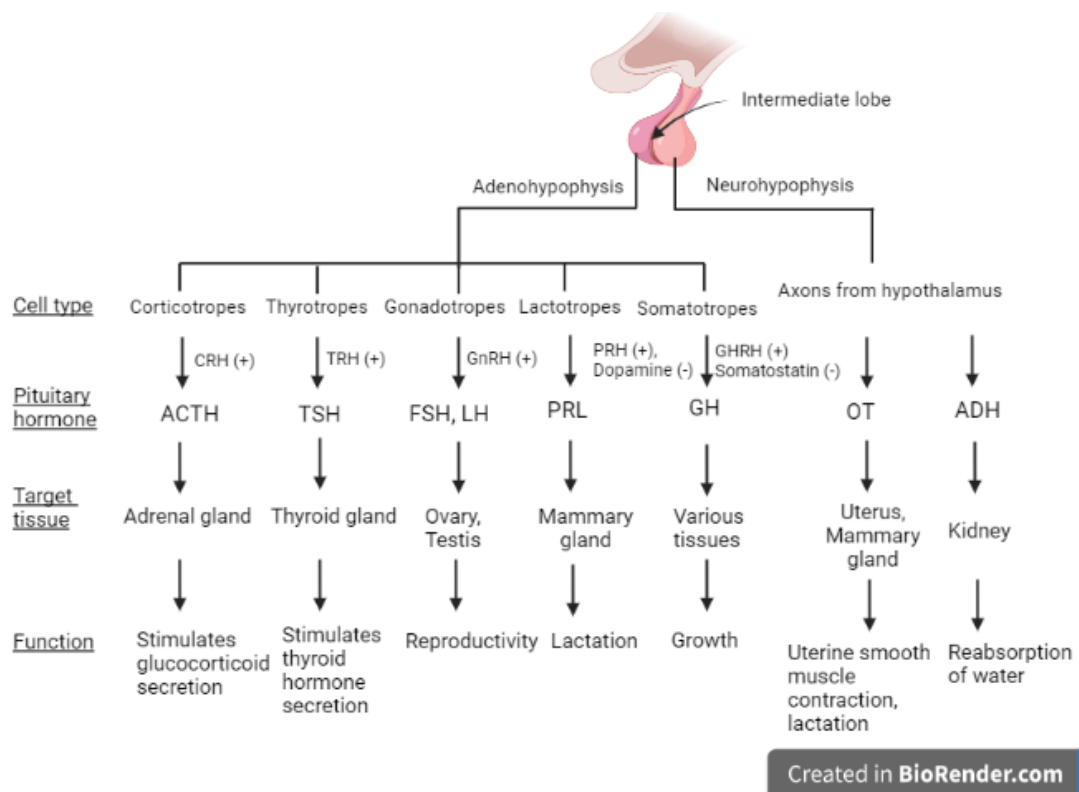
Figure 5. The secreting function of the pituitary gland relies on hypothalamic hypophysiotropic hormones. Hypophyseal hormones induce (+) or supress (-) hormone secretion from the endocrine cells in the adenohypophysis. Hormones secreted from neurohypophysis are produced by hypothalamus and are released to blood due to action potential in the neuron terminal.

Circulating hormones produced by peripheral organs provide feedback to the hypothalamus of the body's state. With the feedback, hypothalamus regulates the hormone secretion from the pituitary gland. The pathways between hormones and target tissues are controlled by negative and positive feedback loops. The negative feedback loops are commonly used in the regulation of hormone production. In the negative feedback loop, the product inhibits the input of the pathway and prevents the accumulation of hormones. Imbalance in the hormone concentrations in blood can affect body homeostasis negatively. Pathways between the hypothalamus, pituitary and target endocrine gland are referred to as axes. One of the major axis involved regulation of homeostasis and stress responses is the hypothalamic-pituitary-adrenal (HPA) axis. As a response to perturbation in tissue homeostasis or external environment sympathetic nervous system activates

and triggers epinephrine and norepinephrine secretion, which then leads to the activation of the pituitary gland. Other important axes are hypothalamus-pituitary-thyroid (HPT) axis and hypothalamus-pituitary-gonad axis (HPG).

1.2.3   Pituitary adenomas

Pituitary adenomas are enlargements or tumors in the pituitary gland that develop from endocrine cells in the adenohypophysis. Pituitary adenomas are usually benign tumors that do not form metastases. In most cases, pituitary adenomas do not cause symptoms because they remain small (Molitch 2017). At later stages of tumorigenesis, adenomas cause excess hormone secretion, headaches and impaired vision. The impaired vision is caused by a large tumor putting pressure on the optic chiasm. Also, hypersecretion of pituitary hormones can lead to hypopituitarism when overgrown endocrine cell types occupy space from other cell types decreasing their number.

Developed imaging techniques and diagnostic methods have enabled better research of pituitary tumors. Research have discovered that pituitary adenomas are more common than previously thought, being the third most frequent intracranial neoplasm (Aflorei & Korbonits 2014). However, the classification of pituitary adenomas is not comprehensive and epidemiological characteristics are inconsistent (Chen et al. 2021). Due to the versatile composition of endocrine cells in the adenohypophysis, pituitary adenomas cause diverse pathologies. Pituitary adenoma refers to a large number of disease processes than are molecularly and functionally distinct. Pituitary adenomas include prolactinomas, growth hormone -secreting tumors, adrenocorticotropic hormone -secreting tumors, thyroid-stimulating hormone -secreting tumors and non-functioning adenomas (Molitch 2017). Each of the tumor types has a peculiar pathology based on which hormone secretion it affects. Larger pituitary adenomas, macroadenomas, can have detrimental effects on the endocrinology and physiology of the human body. By interfering to the normal function of the adenohypophysis due to hypersecretion of pituitary hormones. The molecular mechanisms behind the tumor progression are still unclear. Classical oncogenes are rarely mutated in pituitary adenomas but overexpression of growth factors, epigenetic silencing of tumor suppressor genes and deregulation of the cell cycle has been observed (Cano et al. 2014).

Genetically engineered mouse models have modelled the pathogenesis of pituitary tumors and are valuable tools in preclinical studies. Retinoblastoma deficient mice (RB-mice) develop pituitary adenomas in high penetration in adults and illustrate the tumor-causing effect of loss of function in tumor supressor gene (Jacks et al. 1992). Retinoblastoma is a cancer that develops to retina, light-sensitive layer of eyes, in humans. Retinoblastomas are diagnosed in young children and

cover 3% of all childhood cancers (Rao & Honavar 2017). Retinoblastoma causes intraocular malignancies and, if left untreated, leads to death. In mice, effects of *Rb* mutation are widely studied and it has been observed not to cause retinoblastoma. Instead, heterozygous RB-mice develop pituitary adenomas as high rates. RB-mice have a knock-out mutation in the genome, which leads to inactivation of the other *Rb*-allele. Disruption of both alleles in mice causes lethal genotype and homozygous recessive mice die during early development (Jacks et al. 1992). Jacks and other (1992) suggest that the disruption of both alleles is fatal due to anemia caused by the disruption of erythropoiesis in the embryonic liver. RB tumor suppressor protein has a crucial role in the regulation of cell cycle. The loss of function in the *Rb*-alleles leads to uncontrolled cell division, which leads to tumorigenesis in the adenohypophysis in RB-mice.

1.3   Macrophage involvement in endocrine system and tumorigenesis

Macrophages reside in the endocrine glands and interact with endocrine cells affecting the endocrine function. In turn, hormones interact with the immune system. Hormones, neuropeptides and neurotransmitters regulate macrophage biology (Jurberg et al. 2018). The HPA axis is well studied in the terms of neuro-immunoendocrine interactions and HPA axis has been shown to have a major role in survival of critical illness (Beishuizen & Thijs 2004). The disruptions in neuro-immunoendocrine crosstalk can lead to a pathological state. Comprehensive understanding of the function of immune-endocrine entirety is not complete.

Pituitary adenomas have been shown to interfere the normal pituitary function causing excessive and deficient hormonal secretion from the adenohypophysis. Tumor microenvironments induce changes in the macrophage anti-tumoral function generating pro-tumoral phenotypes. Macrophage show a transition from tumor supressing actions to actions that induce tumorigenesis. Macrophages that induce tumor development and progression are called tumor associated macrophages (TAMs). The macrophage involvement in tumorigenesis has aroused interest towards macrophages as targets in cancer therapy. Also, the endocrine and immune interactions have been implied in care medicine providing information of endocrine and metabolic alterations in disease (Beishuizen & Thijs 2004).

1.3.1   Macrophage function in the endocrine system

Interactions between immune and endocrine systems are crucial for the development and function of endocrine tissues (Rehman et al. 2021). An imbalance in the neuro-immunoendocrine communication has been shown to lead to pathological conditions (Beishuizen & Thijs 2004).

Macrophages and the endocrine system express bidirectional regulation and communication involving neural components, as neurotransmitters and neuropeptides, creating a complex immune-neuroendocrine system. Macrophages enhance glucocorticoid production, which in other hand regulate macrophage activity and differentiation into subpopulations (Jurberg et al. 2018).

Macrophages are involved in the development and homeostasis of the endocrine glands and perform trophic functions in the tissues (Sheng et al. 2021). In thyroid gland, macrophages have been shown to involve in formation of colloid, an overgrown of thyroid tissue (Sheng et al. 2021). In mouse gonads, tissue resident macrophages are needed to maintain fertility. Also, it has been shown that before ovulation macrophage number increases in ovarian follicle suggesting their contribution to the function of the ovaries (Cohen et al. 1999). Testicular macrophages are needed to spermatogenesis and regulate steroidogenesis (Sheng et al. 2021). Macrophages are located throughout the adenohypophysis. Pituitary gland and macrophages show complex crosstalk involving the feedback loops between peripheral target tissues and the pituitary gland. Interactions between hormone-producing cells and macrophages induce hormone secretion from the cells, thus affecting the function of other endocrine tissues (Rehman et al. 2021). In pathological state, an acute response is to activate adenohypophysis (Beishuizen & Thijs 2004). During an inflammatory state, HPA has a major role in regulating body's stress responses. In prolonged disease, the hormone secretion for the adenohypophysis is reduced and leading to hypocortisolism (Beishuizen & Thijs 2004). Glucocorticoids, secreted by induction of ACTH from the adenohypophysis, have an effect on leucocyte trafficking. The HPA axis is involved in macrophage development and controlled through stress-associated mediators (Jurberg et al. 2018). Also, it is suggested that adrenal resident macrophages may regulate the adrenal function independently from the pituitary regulation (Sheng et al. 2021).

Depletion studies in mice and knock-out mouse lines are useful in order to evaluate the importance of the presence of tissue-resident macrophages for endocrine tissue function and development. Transgenic Csfm[op/op] mouse line has a null mutation in Colony stimulating factor 1 (*Csf1)* gene. CSF1 is a growth factor that stimulates the differentiation, proliferation and viability of macrophages. Csfm[op/op] have abnormalities in endocrine organs and disruption in the negative feedback loop in hypothalamic-pituitary-gonadal axis (HPG axis) due to hormonal imbalance (Pollard et al. 1997) Furthermore, in ovary macrophage deficient mice show prolonged estrous cycles causing infertility, when in testis the testosterone production is decreased (Cohen et al. 1999). It has been shown that in diabetic mouse models, macrophage subsets are significantly altered (Eguchi & Manabe 2013). These studies show that macrophages are involved in the development and function of endocrine tissues. However, studying macrophage contribution in endocrine glands by depletion can be challenging because mouse models lacking CSF1 are

deficient for most macrophage populations (Pollard 2009). Endocrine system involves multiple tissues controlled by the pituitary gland and function through feedback loops, thus the depletion is never tissue-specific. For this reason, it is difficult to show that the effect is due to macrophage depletion in a specific tissue rather than a combined effect of disruption of other endocrine tissues or pathways of the endocrine system.

In critical illness, the endocrine system is disrupted (Beishuizen & Thijs 2004). As a major endocrine gland, dysfunction in the pituitary may dramatically alter body function and health. Abnormalities in the pituitary function occurs generally as inappropriate or unregulated hormonal secretion. Pituitary gland is either too active causing hypersecretion of hormones or not active enough leading hyposecretion. The deficient in pituitary hormone secretion is referred to as hypopituitarism, a condition where pituitary gland fails to produce one or more hormones or hormone production is decreased. The composition of embryonic macrophages and heterogenous macrophage subset in the pituitary gland have not been studied. Because of the interaction of immune and endocrine systems, the knowledge of macrophage involvement in pituitary function in steady state and pathogenesis would be clinically valuable. The spatial information of pituitary resident macrophages and endocrine cells could shed a light for developing pathologies and interconnections of macrophages and endocrine cells. Macrophage depletion has been shown to disrupt functions of endocrine tissues and organs and the role of the pituitary cannot be underestimated for the body's function. As a major endocrine gland, it determines the function of other endocrine glands and then the whole body.

1.3.2 Tumor associated macrophages

Leucocytes respond to cancer cells as foreign objects and are aimed to destroy them. Lymphoid T-cells and natural killer (NK) cells are key players in an immune response against cancer cells. T-cell subset, cytotoxic T-lymphocytes (CTLs), play an important part of killing cancer cells via the release of granules or by driving cancer cells to apoptosis (Farhood et al. 2019). CTLs identify cancer cells based on antigenic peptides presented by major histocompatibility complex class I (MHC I) molecules that cancer cells express (Farhood et al. 2019). NK-cells mediate killing by cell surface recognition of foreign structures. In cancer, the cell surface-receptor composition is altered compared to normal host cells. When NK-cells are activated due to recognition of altered cell-surface, they secret cytokines and cytotoxic enzymes that kills target cells (Peng et al. 2017). Macrophages are contributors of the innate immunity and thus involved in inflammation, wound-healing and pathological states, such as cancer. Their fundamental function is phagocytosis that is one of the functions maintaining tissue homeostasis but also clearing foreign objects, such as

pathogens and cancer cells. When encountering and recognising a cancer cell, macrophages can phagocytose the cancer cell or processed its antigens into short peptides, which macrophages then show to T-lymphocytes via MHC class II receptors. T-lymphocytes are then stimulated leading to activation and to a change in their phenotype.

Tumorigenesis is no exception of a pathological state that increases leucocyte recruitment in infected tissue as an inflammatory matter. However, recent studies indicate that macrophages contribute to tumorigenesis instead of supressing actions (Chanmee et al. 2014; Pollard 2009). Macrophages are highly plastic and respond to external signals. They may change phenotypes as an adaptation to the tissue environment. Microenvironments generated by tumors have shown to supply signals that induce changes in tissue resident macrophage and recruited monocytes to antitumor phenotypes that have various actions benefiting cancer cells leading to tumor growth and formation of malignant tumors. Tumor environment and macrophage response towards it is the major cause of immunosuppression (Jin et al. 2021).

During tumorigenesis, cancer cells induce their own distinct microenvironment inside tissues. Tumor microenvironment consists of cancer cells, stromal cells and extracellular matrix (ECM) components that involve macrophage and monocyte recruitment. Solid tumors recruit immune cells into the microenvironment with various factors, chemoattractants and hypoxic condition increasing macrophage number compared to steady state. Chemoattractants are molecules that attracts cells to migrate towards the source. Soluble factors derived from the tumor microenvironment, such as cytokines, chemokines and growth factors regulate macrophage recruitment into tumor. The chemokine (C-C motif) ligand 2 (CCL2) has shown to induce recruitment of TAMs and assists metastasis (Jin et al. 2021). In the tumor microenvironment, macrophages change their antitumor phenotype to phenotypes that enhance tumor growth and malignancy of tumors (Chanmee et al. 2014; Pollard 2009).

In advanced cancer, uncontrolled proliferation of cells results in areas running out of oxygen. Macrophages and monocytes are attracted to hypoxic areas. The recruitment due to hypoxia to the cancer microenvironment is referred as hypoxia-induced recruitment. Hypoxia-induced recruitment occurs through release of factors that induce macrophage migration to hypoxic areas. It has been shown that vascular endothelial growth factor A (VEGF-A), endothelin-2 and lactate play a part in the recruitment (Zhang et al. 2021; Chanmee et al. 2014). Angiogenesis in malignant tumors supports rapid tumor growth by providing oxygen and nutrients to cancer cells. After the macrophage recruitment to the tumor microenvironment, the environment induces changes in the phenotypes directing macrophages towards the antitumor phenotypes (Chanmee et al. 2014). Peng and others' (2017) study of human gastric cancer suggests that TAMs impair NK-cell

function and decrease their amount leading to poor patient survival. Lactate concentration is increased in hypoxic regions due to anaerobic metabolism of cells and it has been shown to drive macrophages towards the harmful phenotypes (Zhang et al. 2021).

Studies have provided results of tumor-promoting functions of macrophages in multiple cancer types (Duan & Luo 2021; Peng et al. 2017; Williams et al. 2016). It has been shown that macrophage number increases in pituitary adenomas in humans (Lu et al. 2015). The increased number of macrophages correlates positively with tumor size and invasiveness, but it is adenoma type dependent which macrophage subsets show significant increase in the tumor microenvironment (Lu et al. 2015). This suggests that distinct macrophage subsets contribute progression of different endocrine cell type adenomas. Principe and other (2020) conducted study in the environment generated by pituitary neuroendocrine tumors (PitNETs). PitNETs are common tumors that develop in the adenohypophysis and are classified morphofunctional types based on pathology. They discovered that gonadotrope tumor cell lines recruited macrophages through CSF1 when somatotroph cell lines seemed to use preferably CCL5 in recruitment (Principe et al. 2020). Also, alterations in expression of VEGF and other growth factors have been reported in pituitary adenomas (Cano et al. 2014).

Cancer immunotherapy is rapidly increasing in cancer treatment. Immunotherapy is a treatment for a disease that involves the modulation of the immune system. Immunotherapy is divided into passive and active parts. Passive immunotherapies include blocking antibodies that aim to neutralize the tumor cells and antibodies that induce activation of the immune system against cancer cells. Also, the TAMs can be specifically depleted by targeting them by antigens conjugated with immunotoxins. In active immunotherapy, tumor-specific immune response is generated for example with a cancer vaccine. As a step of developing therapeutic strategies, the involvement of macrophages can be studied in a pathologic state by utilizing mouse models. There are multiple macrophage depletion studies that have shown a delay in tumor progression, inhibition in metastasis and suppression angiogenesis when macrophages are not present in tumorigenesis (Duan & Luo 2021). The results from depletion studies support the involvement of TAMs in tumor pathogenesis. Retinoblastoma deficient mice can be utilized to study macrophage subsets in adenoma progression *in vivo*. Macrophage subsets can be followed through non-tumor state to clear-tumor state in heterozygous RB-mice to identify contribution of certain phenotypes in tumorigenesis and evaluate the effects of the tumor microenvironment.

1.4 Aims

The origin of tissue-resident macrophages in the pituitary gland is not known. The hypothesis is that pituitary-resident macrophages have multiple origins consisting of embryonic and bone marrow-derived macrophages. However, pituitary's location under the brain attached to hypothalamus but outside the blood-brain barrier creates unique immunological environment. To determine the origin or origins of pituitary macrophages, cell fate-mapping studies using tamoxifen-inducible reporter mice will be made. The possible change of the composition of tissue-resident macrophages during the development of a mouse from 17.5-days-old embryo to puberty and into the adulthood are also studied. In the kinetic study, wild type mice will be used and in a comprehensive follow-up of the pituitary macrophage compartments through mouse development until aged of 8 weeks.

To shed a light to the interactions between immune and endocrine systems and to determine the presence of macrophages in all studied time points, spatial relations between LH and GH - producing endocrine cells and macrophages in the pituitary gland are studied. Pituitaries are stained using whole-mount protocol that able the visualization of the whole gland and then imaged with a confocal microscope. Also, adequacy of semi-squash staining technique in 3D imaging of the pituitary gland is evaluated.

To shed a light to on the functionality of pituitary-resident macrophages, macrophage subpopulations are studied in pathological state. Study is conducted with Retinoblastoma deficient mice from no-symptoms phase to clear-symptom phase to investigate, does the tumor microenvironment have an effect on the composition of macrophage observed in steady state. Also, histological stainings are done to evaluate tumor progression between no-symptom phase and clear symptom phase.

This master's thesis has three specific aims:

1.   *To determine the origin of macrophages in the pituitary gland.*
2.   *To investigate the spatial relationship of hormone-producing endocrine cells and macrophages.*
3.   *To study the significance of macrophages in the development and progression of adenomas.*

2 Materials and methods

2.1 Mouse models

In this master's thesis, multiple mouse models were used (Table 1). All mice were kept in Animal Central Laboratory in University of Turku. Mice were bred and housed in specific pathogen-free conditions and under controlled environmental conditions at temperature +21 °C ±3 °C, humidity 55 % ±15 % and 12/12 h light cycle. All experiments were regulated according to the Finnish Act on Animal Experimentation (497/2013). Animal experiments were conducted under the revision and approval of the Regional Animal Experiment Board in Finland, according to the 3R-principle and under Animal license number 14685/2020. Mice had food and water *ad libitum*. Vaginal plug formation was used to determine the time of fertilization in studies that were conducted in 17.5-days-old embryos. Mice are nocturnal animals and mating takes place during the night. The morning when vaginal plug formation was observed was stated as E0,5.

Table 1. Mouse models and methods used in the three aims of this thesis

Mouse model	Aim	Method
C57BL/6NRj	1. *To determine the origin of macrophages in the pituitary gland.*	*Kinetic analysis* *Flow cytometry*
	2. *To investigate the spatial relationship of hormone-producing endocrine cells and macrophages.*	*Immunohistochemical staining* *Confocal imaging*
Cx3cr1^{CreERT2} x Rosa26-EYFP	1. *To determine the origin of macrophages in the pituitary gland.*	*Cell-fate mapping* *Flow cytometry*
Retinoblastoma deficient mice	3. *To study the significance of macrophages in the development and progression of adenomas.*	*Flow cytometry* *Histological staining*

2.1.1 C57BL/6NRj mouse line

C57BL/6NRj (6N, Janvier lab) is an inbred mouse line that is widely used as a wild type (WT) mouse. In this thesis, C57BL/6NRj were used from embryonic E17.5 to 8 weeks-of-age to study

the kinetics of macrophage subpopulations. In addition, C57BL/6NRj were used in imaging to study spatial relationships of macrophages and endocrine cells in the pituitary gland.

2.1.2 Crossing of *Cxr3cr1*^{CreERT2} and *Rosa26-EYFP*

To follow the fate of yolk sac-derived macrophages and their progeny in the pituitary gland, reporter mice with cre/loxP-construct (see page 4) were used. Cx3cr1^{CreERT2} (stock 020940, Jackson Laboratory) male mice were crossed with Rosa26-EYFP (R26R-EYFP; stock 006148, Jackson Laboratory) female mice for our purpose. Rosa26-EYFP mice express Enhanced yellow fluorescent protein gene (*Eyfp*) in Gt(ROSA)26Sor-locus ,but its transcription has been inhibited by two constructs of *loxP*-flanked on either side of a STOP sequence. Cx3cr1^{CreERT2} mouse line co-express tamoxifen-inducible Cre-ER fusion protein and the Cre-recombinase in CX3CR1 expressing cells. In the crossing, Cre-recombinase deletes the STOP sequence via homologous recombination which leads to production of the YFP in the offspring. Furthermore, the yolk sac-derived cells can be labelled in a time-specific manner by inducing the pregnant female at E9.5 with a single dose of tamoxifen. The tamoxifen administration leads to a robust YFP signal in the labelled cells. As a summary, CX3CR1 expressing cells, macrophages, are fluorescent in the offspring and the fate off tamoxifen labelled cells can be determined.

Tamoxifen was used *to label time-specifically and amplify* the YFP-signal in the yolk sac-derived macrophages. Tamoxifen solution was prepared by dissolving 60 mg Tamoxifen (T5648-1G, Sigma-Aldrich) to 100 µl of 99,5 % ethanol and then adding 1,9 ml of rapeseed oil. Solution was sonicated in +37°C water bath for 15-45 minutes until there were no visible crystals. Tamoxifen was stored at -20°C. Progesterone (P0130-25G, Sigma) was injected with tamoxifen to maintain pregnancy. Single dose of 1.5 mg tamoxifen and 0.75 mg progesterone were injected intraperitoneal to pregnant mice at E9,5. At E9.5, the yolk sac is the only structure producing macrophages, which means that with the crossing, the induction causes permanent fluorescent in CX3CR1-expressing cells and their progeny. Tissues were collected at E17.5 and processed to flow cytometry

.

2.1.3 Retinoblastoma deficient mice

RB-mice were used to study the functionality of pituitary-resident macrophage between steady and pathological states. Retinoblastoma is a tumor suppressor gene and as heterozygous (*Rb*$^{+/-}$), RB-mice will develop a pituitary adenoma in 90% probability in adulthood due to the loss of function in the other *Rb*-allele (Jacks et al. 1992). For the study, litters were genotyped to identify

heterozygous ($Rb^{+/-}$) and wild type ($Rb^{+/+}$) genotypes. $Rb^{+/+}$ mice were used as control animals. In $Rb^{+/+}$ mouse, both Rb-alleles are present, and the mouse is considered as a wild type.

The aim was to investigate the relative proportions of macrophage subpopulations in the development and progression of adenomas from the no-symptom phase (2-months-old mice) to the clear-symptom phase (6-months-old mice). Pituitaries were collected from 2-months and 6-months-old WT and heterozygous males. Flow cytometric analyses were performed to evaluate changes in the proportions of macrophage subsets between WT mice and RB deficient mice. To evaluate tumor progression and to support our findings in flow cytometric analyses, histological stainings were performed.

2.2   Flow cytometry

Flow cytometry is a laser-based method that is used to characterize single cells or other particles from suspension based on light scattering properties and emission of fluorescent-conjugated antibodies. For flow cytometry, tissues are processed to a single-cell solution and the single-cell solution is stained with a variety of antibodies that bind to specific cell surface antigens or intracellular components. With designed antibody panels, emissions on different wavelengths of marker-specific fluorescent conjugated antibodies can be utilized to measure several parameters simultaneously. Based on light scattering and the fluorescent signal of specific markers, distinct cell populations can be identified.

Stained single-cell solution is run with a flow cytometer. Flow cytometer consists of fluidic system, optics system and electronic system (Delay & Rieger 2019). Fluidic system moves cells from the stained sample to optic system. The fluidic system pressurises the running buffer to accomplish focused flow where cells line up and are detected one cell at the time in interrogation point. The optic system excitates the fluorochromes with lasers. Lasers are directed into interrogation points to produce fluorescent light signals. Lasers excite fluorochromes of labelled cells in various wavelengths, generating emissions of visible light. Emission signal of the fluorochrome is directed to a specific detector through bandpass filters. The optic system amplifies and collects the emission signal. Emission signals are used to analyse the sample and the electronic system converts the emission signals into voltage pulses. Voltage pulse indicates the observed signal intensity of studied fluorochrome indicating marker expression on cell-surface.

Flow cytometry was used to determine the origin of pituitary macrophages (aim 1) and to evaluate the significance of macrophages in the development and progression of adenomas (aim 3). BD LSRFortessa™ Cell Analyzer was used to detect the distinct composition of marker expressions in the cell suspension in BD FACSDiva™ Software (version 8, Becton Dickinson). Flow cytometry data were further analysed in FlowJo-sofware (version 10, Treestar Inc.).

2.2.1 Sample collection

To study the origin of pituitary macrophages, pituitaries and spleens were collected at E17,5, newborn, 1 week, 2 weeks, 5 weeks and 8 weeks of age. To investigate the possible effects of tumorigenesis on macrophage populations in RB-mice, pituitaries and spleens were collected in at 2-months-old and 6-months-old. To evaluate labelling success of yolk-sac derived macrophages in cell-fate mapping experiments, brains were collected as a positive control at E17.5. As an exception at E17.5, whole litter was collected to ensure a large enough number of cells to be analysed. Otherwise, only males were used to avoid possible effects of cyclic variation in hormone levels that occur in female mice.

For tissue collection from E17.5 embryos, pregnant females were sacrificed by CO_2 asphyxiation and cervical dislocation. Uterus was dissected and placed to ice-cold phosphate buffered saline (PBS) for 30 minutes to cause hypothermia that euthanizes the embryos. Embryos were dissected from the uterus and decapitated. Pituitaries were dissected from the skull and one litter was pooled into one sample. Newborn mice were euthanized by decapitation because of their resistance to hypoxia. 1-week-old mice were first anesthetized with Isoflurane (170579, Attane vet) and then decapitated. Detached heads were placed to a 24-well plate to ice-cold PBS. Mice of two weeks and older were sacrificed by CO_2 asphyxiation and cervical dislocation. Pituitary glands were dissected from the skull and placed to 900 µl ice-cold Hank's Balanced Salt Solution (HBSS; RNBF2378, Sigma-Aldrich) on a 24-well plate. Until two weeks of age, pituitaries were pooled to ensure a large enough number of cells to be analysed and the amount of pooled individuals was optimized for each time point. For flow cytometry, tissues were processed to single-cell suspensions and stained with antibody mixes.

2.2.2 Isolation of pituitary and spleen macrophages and brain microglia

Pituitaries were mechanically lysed by suspending. 50 µg/ml Dnase 1 (D4527, Sigma,) and 1mg/ml Collagenase D (1-088-874, Roche) were added and incubated for 30 minutes at +37 °C. Solution was suspended again and filtered through silk (pore size 77 µm). Cell suspension was

pelleted (1006G, 1.5 minutes) and washed with 500 µl of HBSS to remove enzymes. Cells were eluted to 300 µl of HBSS for the final volume.

Spleens were used as a control tissue for the staining. In embryonic and newborn time points, three spleens were pooled into one sample. Spleens were collected to 1 ml of PBS on ice. In embryonic and newborn time points, spleens were mechanically lysed by suspension. At later time points spleens were minced through a metal mesh using the plunger of 1 ml syringe. Mesh was washed with 1 ml PBS and the cell suspension was collected and pelleted (1006G, 1.5 minutes). To remove red blood cells from suspension, cells were lysed with a NaCl-treatment by first adding 1 ml 0,2% NaCl and vortexing 15 seconds and then adding 1 ml 1,6% NaCl. Cell suspension was pelleted (1006G, 1.5 minutes) and washed with 1ml PBS. Cells were eluted varying amounts of PBS to adjust the cell density of the sample (500 µl E17.5 and newborn, 1000 µl 1-2 weeks and 1500 µl from 5 weeks onwards). Suspension was filtered through 77 µl silk.

Individual brains were collected to 900 µl HBSS on a 24-well plate. Brains were minced with scissors and incubated with Dnase1 (50 µg/ml) and Collagenase D (1mg/ml) for 20 minutes at +37 °C. Immediately after incubation, brains were homogenized by suspending with a pipet. Cell suspension was collected and centrifuged 300G for 5 minutes. Supernatant was removed by pipetting. Percoll method was used to separate microglia from cell suspension. First, "100%" Percoll was prepared by mixing 1:10 10xPBS (BP399-4, Thermo Fisher Scientific) and Percoll solution (17-0891-01, GE Healthcare). Then "100%" Percoll was used to prepare 70% and 30% Percoll in PBS and 37% Percoll in HBSS. HBSS in 37% Percoll was used to create a layer of different colour between 70% and 30 % gradients to enable the collection of microglia between the layers. Gradients were created into 1.5 ml tubes by first pipetting 400 µl of 30% Percoll to the tube. 400 µl 37% Percoll was pipetted under 30% Percoll. Pellet from homogenized brains was mixed with 400 µl with 70% Percoll solution and was pipetted under 37% Percoll. Samples were centrifuged at 500G for 30 minutes at RT without brakes. Microglia form a distinct intermediate layer between 70% and 37% Percoll gradients. 400 µl of the intermediate layer between the gradients was collected. 400 µl PBS was added and centrifuged (1006G, 1.5 minutes). Supernatant was discarded and the final sample volume was adjusted to 100 µl by adding PBS.

2.2.3 Antibody-staining of cell-surface markers

To study composition of embryonic and bone marrow-derived macrophages in various time points, single-cell solutions were stained with designed antibody mixes (Supplement 1, tables 1.-

4) and analysed with flow cytometry. Three antibodies were used in the analyses: CD45, F4/80 and CD11b. F4/80 and CD11b are commonly used in the study of macrophage origins.

Cell suspension was transferred to a 96-well plate. Cells were pelleted (1500 rpm, 3 minutes, Eppendorf Centrifuge 5810 R). After pelleting, cells were stained with a LIVE/DEAD -stain (Fixable Viability Dye eFluor™ 780, eBiosience) diluted 1:1000 to PBS. LIVE/DEAD-stain was incubated 15-20 minutes in the dark on ice. After incubation, cells were washed twice 200-250 µl with EPICS I (Supplement 1). Fc-receptors were blocked for 5 minutes on ice by using 10 µl purified anti-CD16/32 (CUSTOM24G2, BioXcell) diluted 1:100 in EPICS I to reduce the non-specific binding of the antibodies. Cells were stained with 100 µl antibody mix and incubated for 30 minutes in the dark on ice. Antibody dilutions are presented in the supplementary material (Supplement 1, tables 1.-4.). Each staining included an unstained control well where 100 µl EPICS I was added instead of antibody mix. The control well was used to exclude autofluorescence of the cells in the analyses. Cells were washed twice with EPICS I. Finally, cells were eluted to 250 µl of FACS FIX (Supplement 1) or EPICS I and stored at +4°C covered in foil. Reporter samples were run on the same day and eluted to EPICS I. Otherwise, samples were fixed and run in BD LSRFortessa™ Cell Analyzer within three days from staining.

2.2.4 Statistical analyses

Statistical analyses were performed in GraphPad Prism -software (version7, GraphPad Software). Comparisons between macrophage populations in different time points and *Rb*-genotypes were done by using the unpaired T-test or Mann Mann-Whitney U -test. For embryonic and newborn time points unpaired T-test was used, otherwise significance was calculated with Mann-Whitney U -test. P-values < 0.05 were considered statistically significant.

2.3 Whole-mount staining

Whole-mount staining is a technique where whole tissue or part of it is stained and cleared for imaging. At first, tissues are stained with antibodies and then cleared into transparent. The technique allows imaging of the tissue structure in 3D. The technique is well suited for imaging pituitary structure and cell localisation because the gland can be stained as a whole. Whole-mount stainings were performed to show the presence of macrophages through the development of mice and further to visualise the spatial relationships of macrophages and endocrine cells in the pituitary gland.

2.3.1 Sample collection

Pituitary glands were collected from C57BL/6NRj male mice at E17,5, newborn, 1 week, 2 weeks, 5 weeks and 8 weeks of age. Pituitaries were dissected attached to the skull to prevent the gland from braking. Samples were fixed in 2% paraformaldehyde (PFA; sc-281692, Santa Cruz Biotechnology) in PBS for 20 minutes on ice. Samples were washed in PBS (3x 10 min) at +4°C shaking. Between the second and third wash pituitary was dissected from the skull. Samples were dehydrated in a graded series of methanol and then stored in 100% methanol at –20 °C.

2.3.2 Immunohistochemical staining and clearing

Samples were rehydrated in 50% methanol (MeOH) in PBS for 20 minutes on ice and twice in PBS for 20 minutes on ice. Before staining, samples were blocked for 6 hours in blocking solution (Supplement 2) at +4°C shaking to reduce the unspecific binding of antibodies. To show the presence of macrophages in mice pituitaries, double-staining was performed. A general macrophage marker, F4/80, was used to identify pituitary-resident macrophages. To facilitate the visualization of the three-dimensional structure of the gland, a pan-endothelial marker MECA-32, was used. MECA-32 binds to vascular endothelium and ables the visualisation of pituitary vasculature improving the 3D-view. To study endocrine cells in relation to macrophages, a hormonal antibody was added to the described double staining. Antibodies for LH and GH were tested in triple-staining. Somatotropes are the most common cell type in the pituitary gland when gonadotropes are found in various locations (Ooi et al. 2004). Based on these facts, the two endocrine cell types were chosen because they were thought to be convenient to image.

Staining was performed in a 96-well plate in 100-200 µl volume. Primary antibodies (Table 2) were diluted to washing solution (Supplement 2) and secondary and conjugated antibodies (Table 3) were diluted in blocking solution (Supplement 2). After blocking, primary antibody mixes were added and incubated overnight at +4°C shaking. Samples were washed 3 times for 2 hours in washing solution at 4°C shaking. After washes, secondary antibodies were added and incubated overnight at +4°C shaking covered in tin foil. Washes were repeated and conjugated antibody was added and incubated overnight at +4°C shaking covered in tin foil. Washes were repeated and sample were rinsed 3 times for 20 minutes with 0.4% Triton in PBS on ice. Samples were dehydrated through graded MeOH series on ice, first in 50% MeOH for 20 minutes and then twice in 100% MeOH for 10 minutes. Samples were stored in 100% MeOH at +4°C covered in tin foil until clearing.

Table 2. Primary antibodies used in whole-mount staining

Antigen	Target	Host species	Manufacturer & catalog number	Dilution
F/80	Macrophages	rat	Bio X Cell, BE0206	1:500
LHb	LH	rabbit	NIDDK, AFPC697071P	1:1000
GH	GH	rabbit	NIDDK, AFP5672099	1:1000

Table 3. Secondary antibodies and conjugated antibody used in whole-mount staining

Fluorochrome	Host species	Reactivity	Manufacturer & catalog number	Dilution
A546	goat	rat	Life technologies, A11081	1:200
A647	goat	rabbit	Invitrogen, A27040	1:100
MECA-32-A488	rat	Endothelium of blood vessels	BioLegend, 120506	1:50

For clearing 50% and 100% BABB solution were used. 100% BABB was prepared by mixing 1:3 Benzyl alcohol (402834-100ML, Honeywell) and 2:3 Benzyl benzoate (B6630-250ML, Sigma-Aldrich). 100% BABB was used to prepare 50% BABB. For 50% BABB 100% methanol and 100% BABB was mixed 1:2. Samples were placed to 35 mm Petri dishes with a glass bottom. Samples were cleared twice with 100 µl 50% BABB for 15 minutes. 50% BABB was replaced with 100 µl 100% BABB. 100% BABB treatment was repeated three times with 10 minutes of incubation. Finally, 100% BABB was changed to a new 100% BABB and samples were mounted with a cover glass. Samples were stored at +4°C in the dark until imaging. Imaging was performed within a week from clearing.

2.3.3 Imaging and analysis

Imaging was performed using an LSM880 confocal microscope (Zeiss) with an Axio Observer.Z1 microscope using ZEN 2.3 SP1 black edition acquisition software at RT. The objectives used were a Zeiss C Plan-Apochromat 20x/1.4 without immersion and Zeiss C Plan-Apochromat 40x/1.2 with water immersion. For further image processing, ImageJ was used.

2.4 Semi-squash staining

Semi-squash is a technique where tissue structure slightly breaks down to allow antibodies to penetrate the tissue. In semi-squash, the pituitary gland can be stained as a whole. Semi-squash staining was performed to evaluate, can this technique be utilized in 3D imaging of macrophages and endocrine cells in the mouse pituitary gland. The technique had not previously been used in imaging the pituitary gland. The collection protocol was optimised for pituitary staining using primary antibodies for LH and GH described before. The optimised protocol is presented below, and the optimising process is discussed later.

2.4.1 Sample collection

Pituitaries were collected from adult C57BL/6NRj male mice. Adult mice were used to ensure the production of the studied hormones. Also, the gland is easier to collect and handle from an adult mouse than from embryos. Pituitaries were dissected from the skull and placed to ice cold PBS on a 24-well plate. Pituitary was moved onto a microscope slide with 70 µl of PBS. Tissue was covered with a coverslip (24x24) to squash the tissue and break its structure slightly. Slide was dipped into liquid nitrogen for 10 seconds. Coverslip was removed by flipping it off. Without delay, tissue was fixed in 90% ethanol for 2 minutes. Slides were air-dried at RT overnight and stored at -70°C.

2.4.2 Immunohistochemical staining

Grease rings were drawn around samples to prevent waste of reagents. Samples were post-fixed with 2% or 4% PFA in PBS for 15 minutes in RT. Tissues were rinsed with PBS and permeabilized with 0.2% Triton-X in PBS for 10 minutes. Samples were rinsed in PBS and incubated in 0,1M NH_4Cl for 15 minutes to decrease autofluorescence. Samples were rinsed in PBS and blocked in 10% bovine serum albumin (BSA) in PBS for 30 minutes at RT. BSA was removed and primary antibody diluted (Table 4) to 10% BSA was incubated overnight at +4°C in a humidity chamber. Samples were washed three times for 5 minutes in PBS shaking at RT. Secondary antibody diluted (Table 5) to 10% BSA were incubated in a humidity chamber at RT for 1 hour. Samples were washed three times for five minutes in 0.05% Tween-20 (93773-250G, Sigma) in PBS at RT shaking and once in PBS at RT shaking. DAPI (D1306, Invitrogen) was used to locate cells in imaging. DAPI (stock 5mg/ml in MilliQ water) diluted 1:5000 in PBS was incubated for 15 minutes in a humidity chamber at RT and rinsed in PBS. Samples were mounted with ProLong™ Gold Antifade Mountant without DAPI (P36930, Thermo Fisher Scientific).

Samples were dried overnight at RT and then moved to +4°C. Imaging was performed within a week from staining.

Table 4. Primary antibodies and PFA used in semi-squash staining

Antigen	Reactivity	Host species	Manufacturer & catalog number	Dilution	PFA-fixing
LHb	Anti-mouse	rabbit	NIDDK, AFPC697071P	1:500	2%
GH	Anti-rat/mouse	rabbit	NIDDK, AFP5672099	1:500	4%

Table 5. Secondary antibody used in semi-squash staining

Fluorochrome	Host species	Reactivity	Manufacturer & catalog number	Dilution
A488	goat	rabbit	Life Technologies, A-11034	1:500

2.4.3 Imaging and analysis

Imaging was performed using a confocal microscope 3i spinning disk (Intelligent Imaging Innovations) microscope equipped with an LD c-451 apochromat 40×/1.1 water objective and SlideBook 6 software (Intelligent Imaging Innovations) at RT. For further image processing, ImageJ was used.

2.5 Histological staining

Hematoxylin-eosin staining (HE-staining) was used to evaluate tumorigenesis in RB-mice at ages 6 and 10 months. HE-staining is a widely used staining method in histological studies. Possible histological alterations due to pathological states can be studied with the staining. In HE-staining tissues, thin tissue sections are stained with two dyes: hematoxylin and eosin. Hematoxylin stains acidic structures (e.g. nucleus) purplish-blue and eosin stains basophilic structures (e.g. cytoplasm) in pink.

2.5.1 Sample collection

Pituitary was dissected attached to the skull and placed to 1 ml of PBS on ice. Pituitaries were fixed with 10 % Formalin (HT501128, Sigma-Aldrich) at RT overnight. After fixing pituitaries were moved to tissue cassettes and dehydrated through graded ethanol (EtOH) series for 1 hour

in 50% EtOH and 30 minutes in 70% EtOH at RT. Samples were stored in 70% EtOH at +4°C. The embedding of tissues was performed by the Histology core facility of the Institute of Biomedicine, University of Turku, Finland.

2.5.2 Sample preparation and hematoxylin-eosin staining

Blocks were cut with RM2255 Automated Microtome (Leica). Sample thickness was adjusted to 5 μm. All steps of the staining protocol were conducted at RT. Paraffin was removed with xylene (28973.363, VWR Chemicals). Samples were incubated 3 times for 5 minutes in xylene. Samples were rehydrated through 2 minutes incubations in decreasing series of ethanol (99.5%, 95%, 70% and 50%) and finally placed to dH_2O for 5 minutes. Samples were placed to Mayers hematoxylin (MS16, Sigma-Aldrich) for 20 minutes. Samples were rinsed for 15 minutes under running warm tap water. Tissues were placed to dH_2O for 30 seconds and moved to 95% EtOH for 30 seconds. Without delay, samples were placed to eosin (180072, Reagena) for 10 seconds. Samples were dehydrated through ascending series of ethanol and finally placed to xylene. Slides were mounted with DPX mountant for histology (06522, Sigma). Slides were imaged with Pannoramic P1000 (3DHISTECH) and analysed with Pannoramic Viewer (Version 1.15.4, 3DHISTECH).

.

3 Results

3.1 Macrophages are present in the prenatal and postnatal pituitary gland

Whole-mount staining was performed to characterize and localize macrophages within the pituitary gland of mouse embryos, neonatal and postnatal mice. Macrophages were stained with F4/80 macrophage marker. To get a better view of the architecture of the tissue and location of macrophages pan-endothelial marker MECA-32 was used to stain the endothelium of blood vessels. Samples were imaged with a confocal microscope and images were further processed in the ImageJ.

Macrophages were present in all studied time points from E17.5 to 8-weeks-old mouse (Figure 6). In whole-mount high-quality images of macrophages in the vascular network were obtained. The morphology and location of macrophages can be observed through the timeseries. E17.5 to 1-week-old mice, macrophages seem to be attached to blood vessels (Figure 6A). In older animals, macrophages show more diverse localisation by being separated from the blood vessels (Figure 6B). The structure of the vascular network developed through the time points of E17.5, newborn and 1-week-old mice (Figure 6A). The structure at E17.5 and newborn seems to be more unorganised and gives a weaker signal than in older animals. Also, careful observations of the morphology of the macrophages can be done. Macrophages underwent morphological changes from spherical to mature cells, showing more complex morphology with multiple dendrites typically found in adult tissues (Figure 6B).
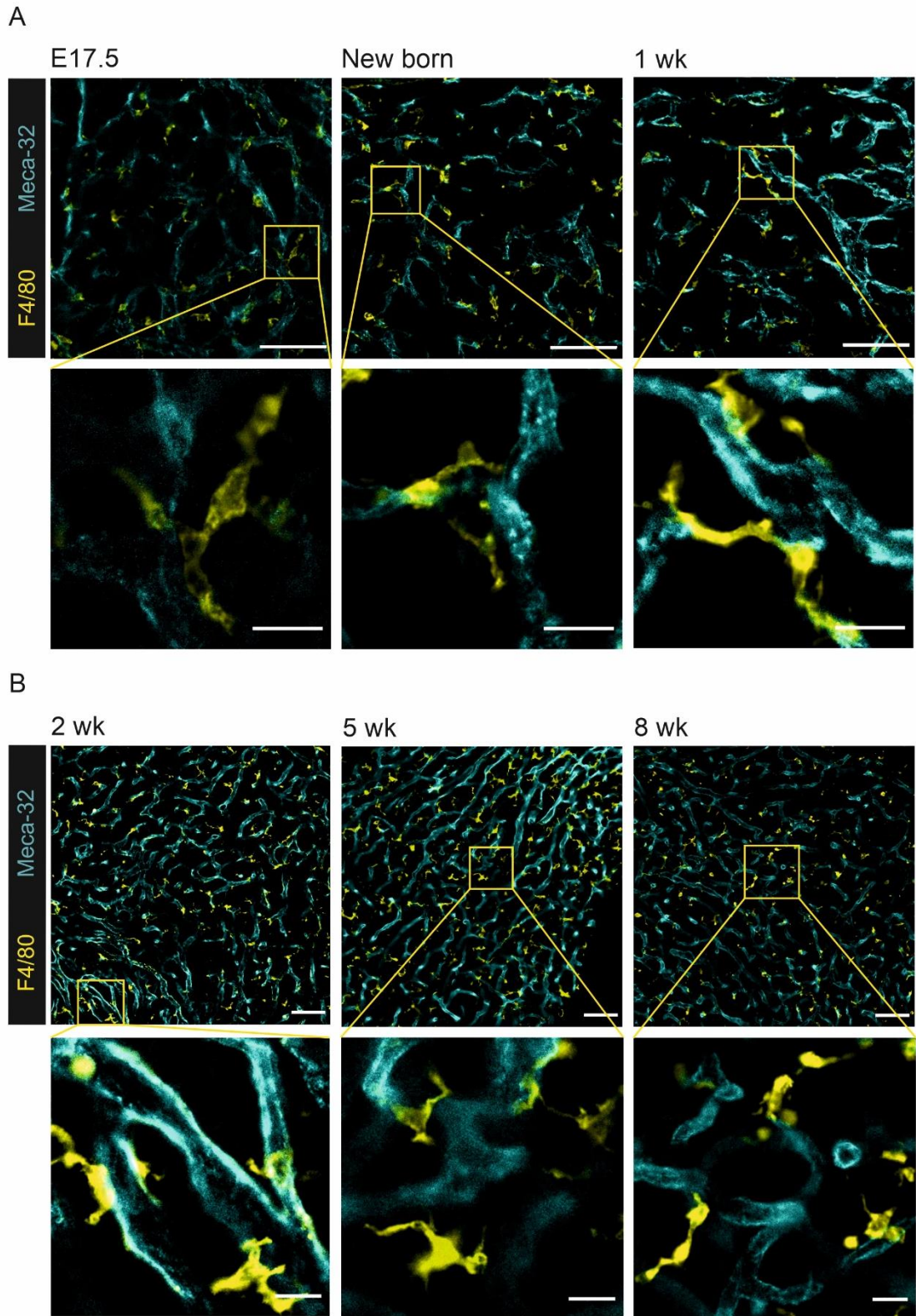
Figure 6. Immunofluorescence staining for pituitary macrophages (F4/80, yellow) and vasculature (MECA-32, cyan) from C57BL/6NRj mice at different time points. A. In earlier time points, macrophages are found attached to blood vessels. MECA-32 signal amplifies as the animal ages, suggesting a more organized structure of the blood vessel. B. From two weeks onwards, macrophages show more diverse localisation and morphology. Scale bars are 50 μm in the upper panel and 10 μm in the lower panel. Images were taken with a confocal microscope and panel A was imaged with 40x water objective and panel B with 20x air objective.

3.2   Visualising LH- and GH-secreting endocrine cells

The aim was to study the localisation of macrophages in relation to endocrine-cell types. After the success in F4/80 and MECA-32 double staining, we performed triple staining by adding a third antibody to visualise hormone-producing cells together with F4/80 and MECA-32. Staining of LH-secreting cells was incomplete and the signal was weak (Figure 7). Adjustments of brightness and contrast were applied to the whole image. The locations of the stained cells followed the results of Davis and others (2011) locating rostral locations of the gland. However, the stained cells were found only in the outermost parts of the rostral pituitary gland, which suggests that antibodies have not properly penetrated into the tissue and staining of cells is restricted on the edges of the tissue. No GH signal was detected in the triple staining and the results are excluded from this thesis.
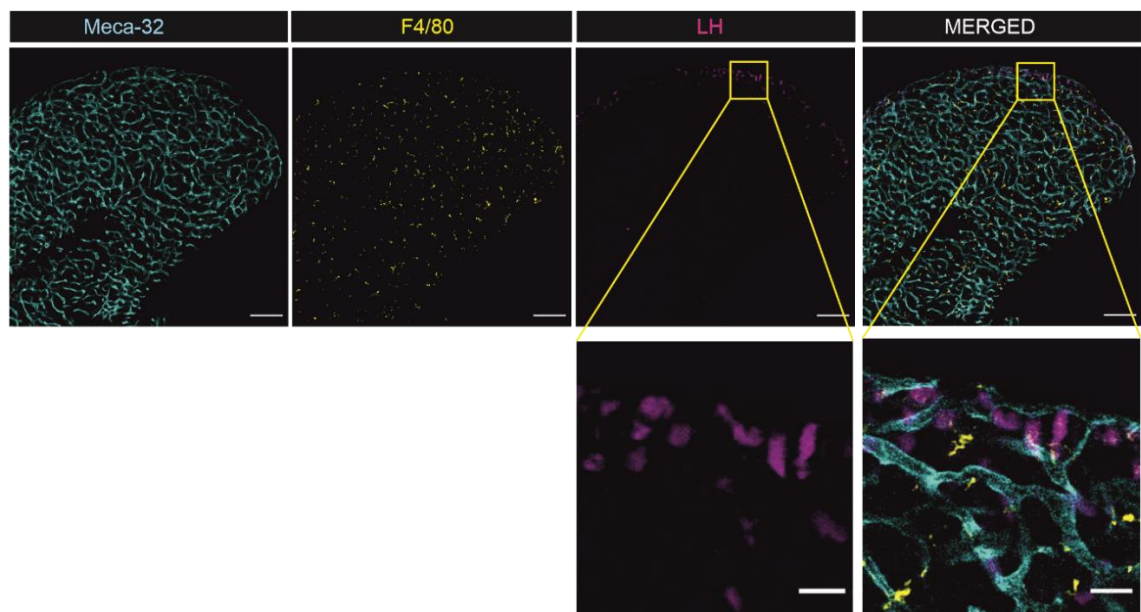

Figure 7. Whole-mount staining of macrophages, blood vessels and LH-secreting cells in 8-weeks-old C57BL/6NRj mouse pituitary gland. Weak signal of LH (magenta) was obtained in the outer parts of the rostral region of the pituitary gland. Staining of blood vessels (cyan) and macrophages (yellow) was successful. Scale bar in the upper panel is 100 μm and in magnification 20 μm.

Because of a poor signal of primary hormonal antibodies in whole-mount staining, semi-squash staining was performed. The technique had not been used before in immunohistochemical staining of the pituitary gland. The tissue collection protocol was optimised and the staining with nuclear marker and primary-secondary staining using one hormonal antibody at a time was tested. Nuclear marker DAPI was used to identify cells. Adult mice, as their pituitary glands are easier to collect and process than embryonic or neonatal ones, were used to ensure hormone secretion.

LH- and GH-secreting cells were visualised in semi-squash staining of 7-weeks-old C57BL/6NRj male mice pituitary glands (Figure 8). Negative controls stained with secondary antibody A488 confirmed that the binding of primary antibodies is specific. Primary LH-antibody did penetrate deeper into the tissue than in whole-mount staining and greater cell-number was observed confirming incomplete staining of the LH-secreting endocrine cells in whole-mount. Distinct location of LH- and GH-secreting endocrine cells was observed. LH-cells were found in the rostral areas but they were also enriched in lateral wings of the gland (Figure 8A). GH-secreting cells were located throughout the gland which is in line with the literature (Figure 8B; le Tissier at al. 2012). Also, we were able to obtain a sufficient amount of stacks that the tissue architecture can be imaged in 3D.
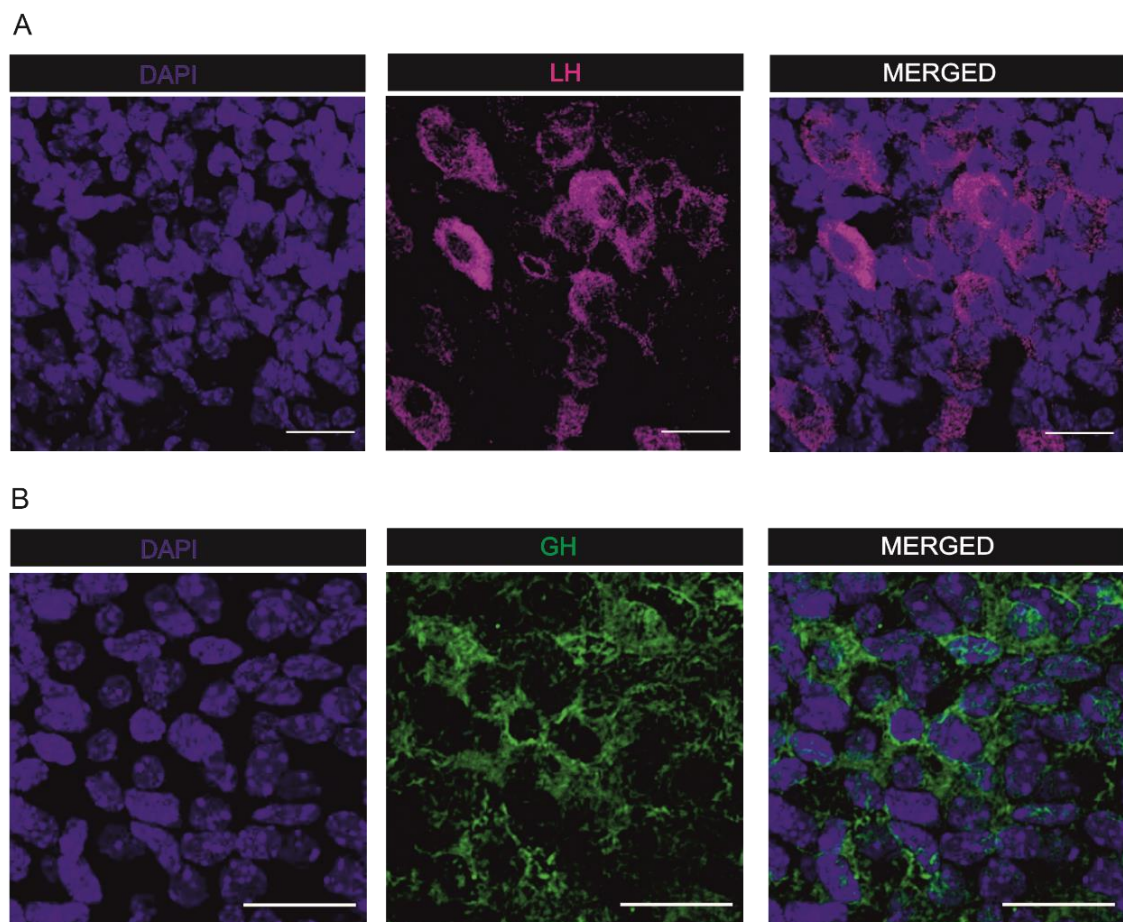

Figure 8. Semi-squash staining of LH- and GH-secreting cells in 7-weeks-old C57BL/6NRj mice pituitary glands. A. LH cells (magenta) were stained in the rostral and lateral locations of the pituitary gland giving a good signal. B. Somatotropes secreting GH (green) were comprehensively stained and showed robust distribution in the pituitary gland. Nuclear marker DAPI is shown in blue. Scale bar is 20 µm. Images were taken with a confocal microscope and 40x water objective.

To exceed the result presented in Figure 8, fixing with PFA for both primary antibodies was adjusted separately, Triton-X concentration was increased to enhance permeabilising of the cell membrane and the incubation time of the primary antibody was extended from one hour to

overnight to increase the binding of the antibodies. However, the suitability of semi-squash in 3D imaging of macrophages in the pituitary gland needs further testing. When the tissue is squashed, the location of macrophages or other cells might shift and distort the spatial relationships.

3.3 Characterisation of pituitary macrophages by flow cytometry

In order to determine the origin of pituitary macrophages and investigate the progression of the tissue-resident macrophage populations, flow cytometry was used. Furthermore, flow cytometry was used to study the influence of tumor microenvironment on adult tissue-resident macrophage populations and evaluate their significance in the development and progression of adenomas.

3.3.1 Gating strategies

The selection of successive subpopulations of cells in flow cytometry is a critical requirement for efficient and reliable analysis. Tissue-resident macrophage populations in the pituitary gland were analysed with FlowJo-software. Two gating strategies were used. Firstly, gating to define macrophage compartments in all time points and secondly, gating to prove that the observed $CD11b^{int} F4/80^{high}$ macrophages population has derived from the yolk sac (Figure 9). Gating A was used to study yolk sac, fetal liver and bone marrow-derived macrophages in all time points in all mouse models used in flow cytometric analyses. Gating B was limited to cell-fate mapping studies in reporter mice.

In Gating A, side-scattering (SSC) and forward scattering (FSC) were used to eliminate dead cells and cell aggregates. Live cells were further gated based on a LIVE/DEAD-marker that stains dead cells and live cells remain negative. CD45+ cells were gated as leukocytes from live cells. Pituitary resident macrophages were pre-gated as CD45+CD11b+. From pre-gated macrophages two different populations were identified based on CD11b+ and F4/80+ signal intensity. The identification of the macrophage origins based on the markers is dependent on the age of the mice and changes between the early time point (E17.5 and newborn) and postnatal timepoints. Yolk sac-derived macrophages express CD11b at the intermediate level when F4/80 expression is high ($CD11b^{int} F4/80^{high}$) throughout the mouse development. Fetal liver-derived macrophages have high CD11b expression when F4/80 expression is on intermediate level ($CD11b^{high} F4/80^{int}$) at E17.5 and newborn and then shift their phenotype (Ginhoux & Guilliams 2016). In postnatal mice, bone marrow-derived macrophages can be distinguished by $CD11b^{high} F4/80^{int}$ expression (Schulz et al. 2012).

Gating B was used to follow the YFP fluorescence signal in tamoxifen-induced offspring of the crossing *CX3CR1^{CreERT2};R26R-EYFP* at E17.5 (Figure 9). Side-scattering (SSC), forward scattering (FSC) and LIVE/DEAD-gating were used similarly to gating A to exclude cell aggregates and dead cells. From live cells, YFP-positive (YFP+) cells were gated and followed through the further gating. From the YFP-positive population, CD45+ leukocytes were gated. From YFP+CD45+ cells, pituitary resident macrophages were pre-gated as CD45+CD11b+ cells. Finally, YFP+CD45+CD11b+ cells were divided into two populations with distinct embryonic origins based on CD11b+ and F4/80+ signal intensities. Gates for CD11b^{int} F4/80^{high} and CD11b^{high} F4/80^{int} were copied from gating A and placed to CD11b+F4/80+ plot in gating B to define are the YFP+ cells in CD11b^{int} F4/80^{high} gate (yolk sac-derived macrophages).
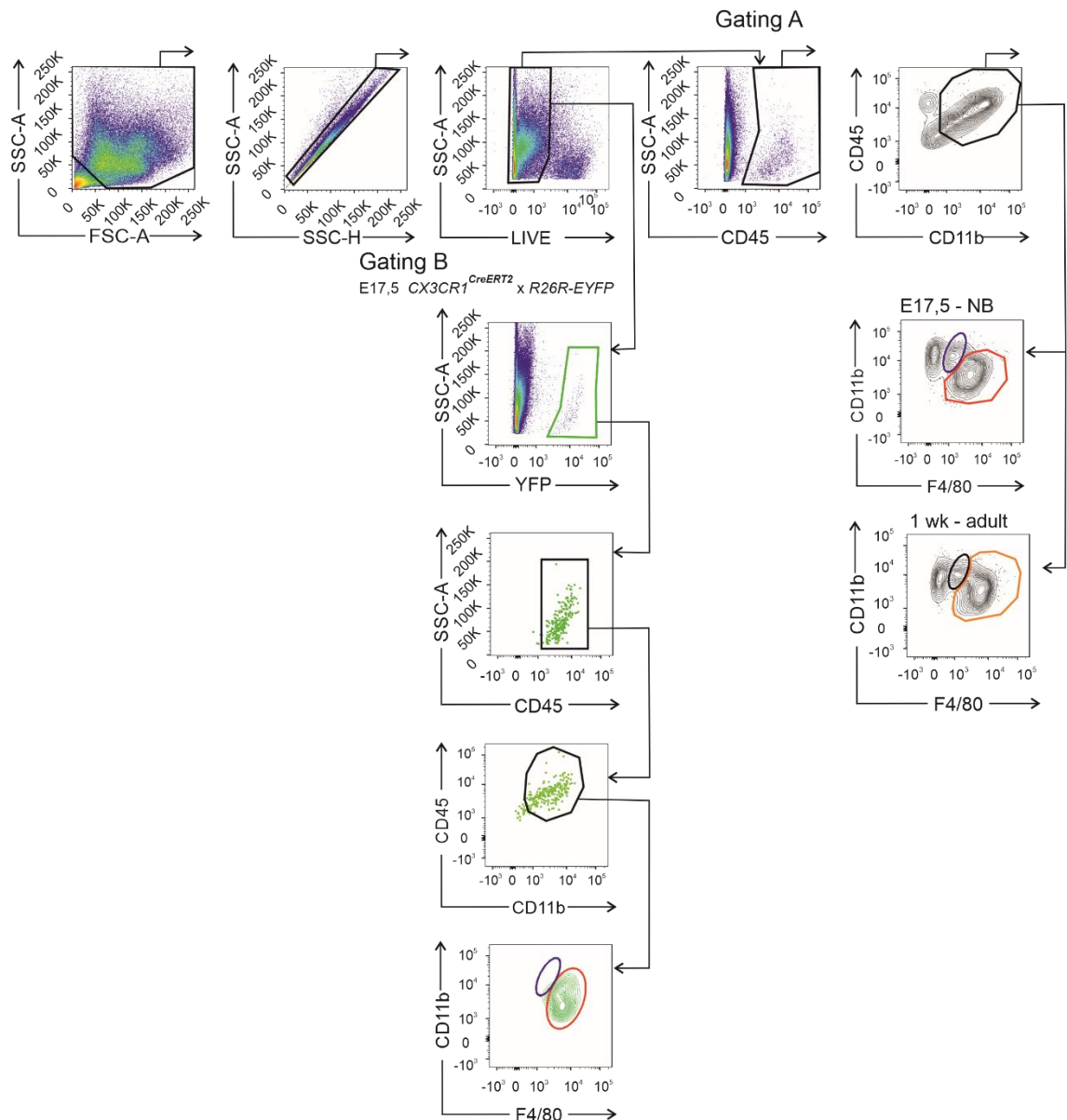
Figure 9. Tissue resident macrophage populations in the pituitary gland were gated using two gating strategies. The two gating strategies separate after identifying live cells. Gating A was used to gate yolk sac, fetal liver and bone-marrow derived macrophages based on CD11b and F4/80 signal intensities in E17.5-newborn (NB) and 1wk, 2wk, 5wk and 8wk timepoints in all experiments. Gating B was used in a cell-fate mapping study to follow the fate of tamoxifen-induced yolk sac-derived cells at E9.5 in E17.5 Cx3cr1[CreERT2] x R26R-EYFP reporter mice. Labelled YFP+ cells are shown in green.

3.3.2 Tissue-resident macrophages are derived from embryonic structures at E17.5 and newborn in the pituitary gland

Two distinct tissue-resident macrophage populations were identified from the embryonic and newborn pituitary. As a result, the tissue-resident macrophage population consists of yolk sac- and fetal liver-derived macrophages (Figure 10A and 10B). The yolk sac-derived macrophages dominate in both time points.
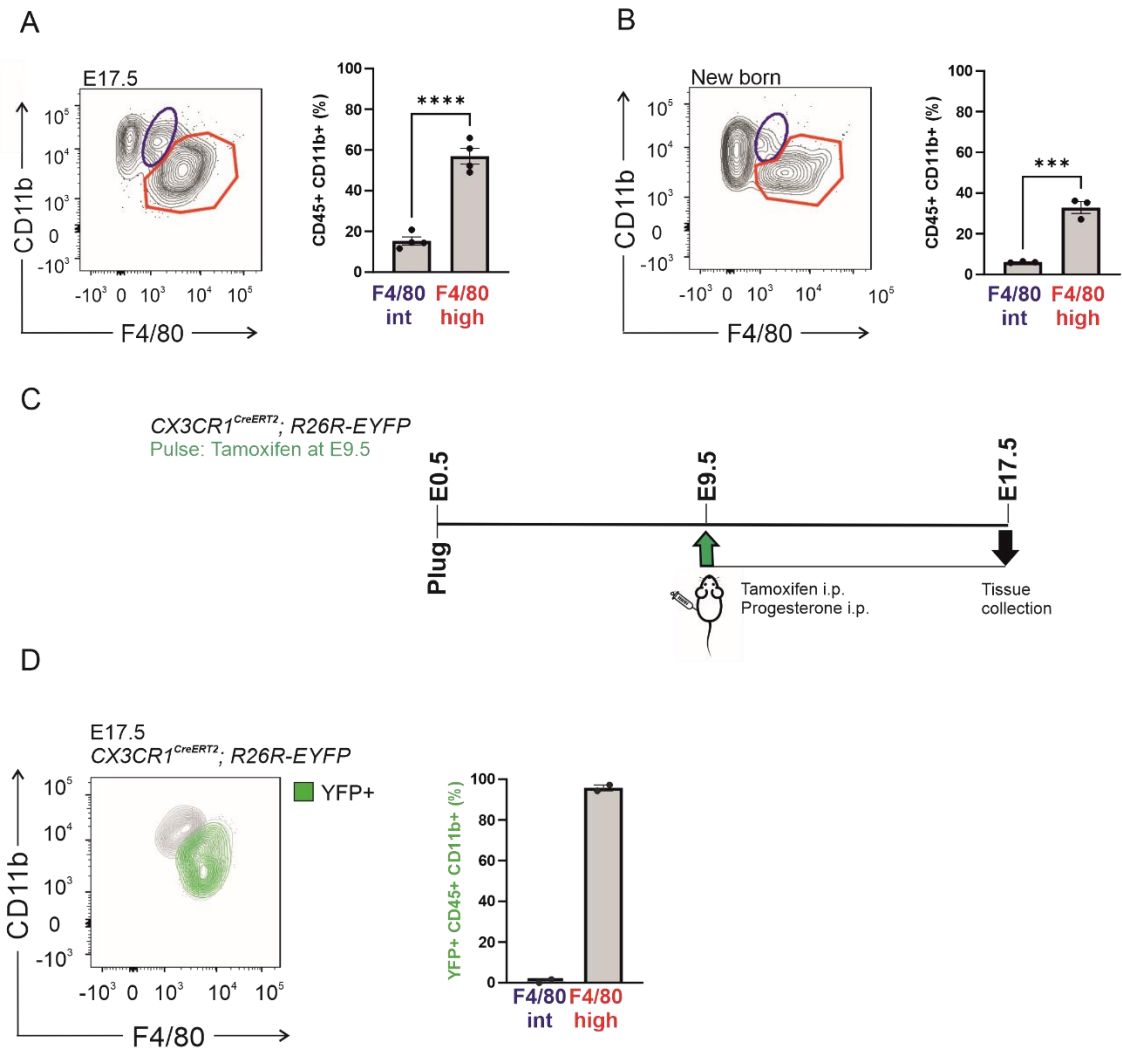
Figure 10. Tissue-resident macrophages derive from the yolk sac and fetal liver in the pituitary gland at E17.5 and newborn mice. A. Flow cytometric analysis of tissue-resident macrophages in the pituitary gland based on CD11b and F4/80 surface marker expression at E17.5 and B. in newborn. The yolk sac-derived macrophages are indicated in red and the fetal liver-derived macrophages are shown in blue. C. Experimental outline of cell-fate mapping study in crossed *Cx3cr1^{CreERT2} x R26R-EYFP* reporter mice. Mice were induced with tamoxifen at E9.5 and tissues were collected at E17.5. D. Flow cytometric analysis of the labelled macrophages showing YFP-fluorescence in *Cx3cr1^{CreERT2} x R26R-EYFP* offspring. The YFP-positive cells are in green. Each dot represents a pool of animals and mean ± SEM are shown. ***p = *0.008,* ****p < 0.0001 (Unpaired T-test)

To show that the dominating population is from the yolk sac, *Cx3cr1^{CreERT2}* male mice were crossed with *R26R-EYFP* female mice and plugged females were injected with tamoxifen at E9.5 to label macrophages in the yolk sac (Figure 10C). Tissues were collected at E17.5 and processed to flow cytometry to analyse the cell fate of labelled descendants. Cells were gated using both gating strategies, A and B (Figure 9). Pituitary macrophages were gated first with gating A. Then same samples were gated with gating B following the YFP+ signal and the final gates from gating A was placed to CD11b F4/80 gate in gating B. CD11b+ F480+ cell populations from gating A and gating B were plotted on top of each other. As a result, almost 100% of tamoxifen labelled

YFP+ cells were CD11b^{int}F4/80^{high} expressing macrophages, proving that the CD11b^{int}F4/80^{high} population derives from the yolk sac in the mouse pituitary gland (Figure 10D). Brain microglia derives from the yolk sac at E8.5, thus, brains were used as a positive control because microglia should be positive for YFP. Microglia expressed YFP-signal confirming the labelling success (Supplement 3).

3.3.3   Bone marrow-derived macrophages infiltrate in the postnatal pituitary gland

In 1-week-old mice, a shift in CD11b and F4/80 expression took place in the pituitary resident macrophage populations. Phenotype of fetal liver-derived macrophages changed and they became CD11b^{int} F4/80^{high} expressing macrophages (Figure 11A). In addition to the phenotypic shift, bone marrow-derived monocytes infiltrated into the pituitary gland. Bone marrow-derived monocytes express CD11b^{high} F4/80^{int} when recruited into tissues and differentiated to tissue-resident macrophages (Figure 11A).

In postnatal mice, pituitary macrophages originated from three different ontogenic sources. From 1 week onwards, macrophages have originated from the yolk sac, fetal liver and bone marrow in the mouse pituitary gland (Figure 11B). At 1-week-old, pituitary gland had recruited bone-marrow-derived macrophages but the population constantly remains as a minor population during the postnatal development. Despite the monocyte infiltration, the yolk sac and fetal liver-derived macrophages were dominating in the pituitary gland and remained as the major population through the postnatal development (Figure 11B).

A

B
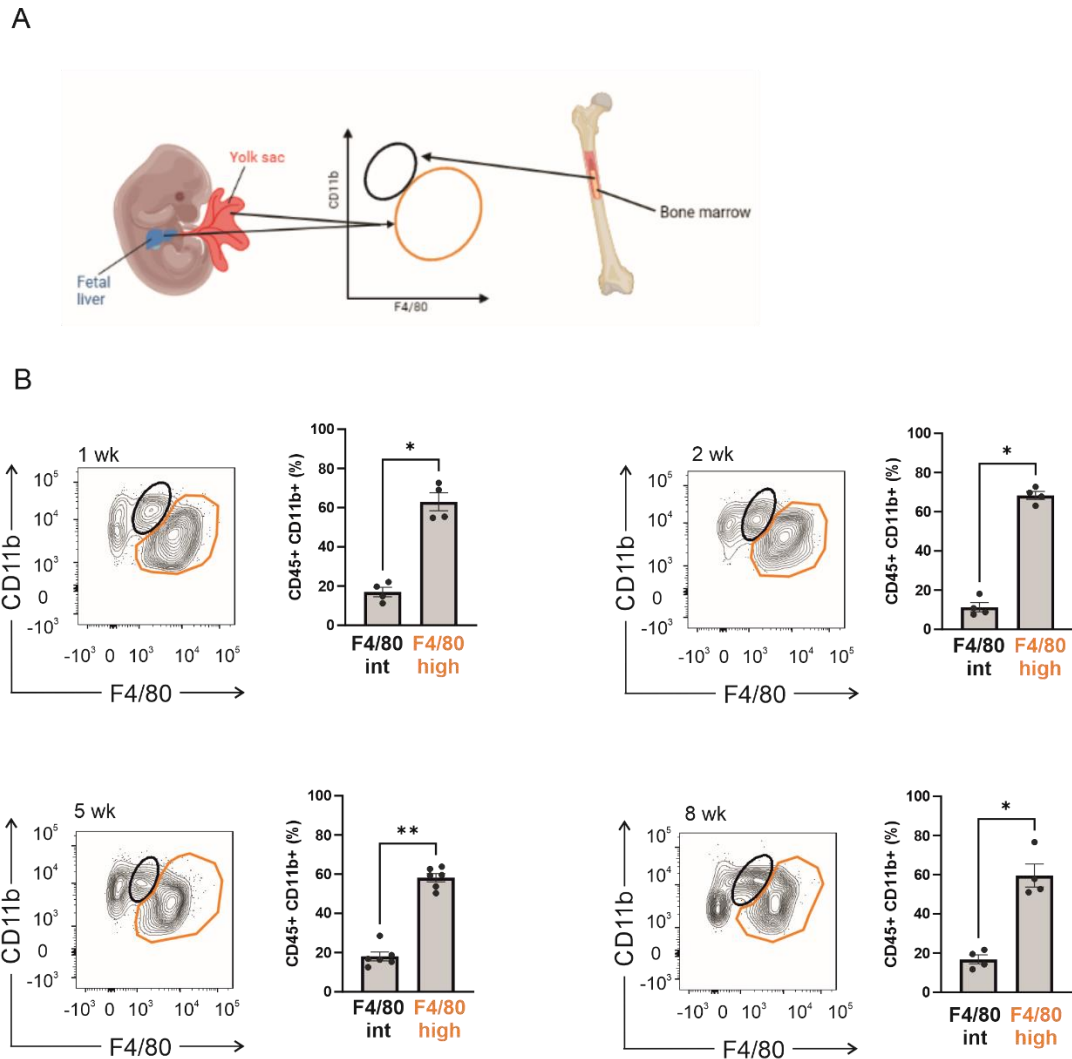
Figure 11. Tissue-resident macrophages consist of embryonic-derived population and bone marrow-derived population in the postnatal C57BL/6NRj mouse pituitary gland. A. A shift in CD11b and F4/80 surface marker expression occurs in postnatal mice. Shift in the expression of the fetal liver-derived macrophages results in one embryonic-derived macrophage population, which includes both the yolk sac and fetal liver-derived macrophages. Bone marrow-derived macrophages infiltrate into the tissue and can be identified by their CD11b^{high} F4/80^{int} expression. B. Macrophages from embryonic origins are dominating the macrophage composition despite the monocyte recruitment. Each dot represents pool of animals (1-2wk) or one mouse (5-8wk) and mean ± SEM are shown. *p =0.0286, **p = 0.0022 (Mann-Whitney U Test). Figure A created in Biorender.com.

3.3.4 Retinoblastoma deficient mice did not show changes in the tissue-resident macrophage populations at 6 months of age in the pituitary gland

For consistency, the CD11b and F4/80 division was used to study changes in macrophage compartments in a pathologic state, tumorigenesis. Pituitaries were collected from 2-months-old and 6-months-old retinoblastoma deficient mice. The embryonic-derived and bone marrow-derived populations were compared between WT *(Rb$^{+/+}$)* and the adenoma-developing genotype

(Rb$^{+/-}$). Comparison was done in the no-symptom phase *(*2 months) and clear-symptom phase (6 months) to study does the adenoma progression at 6 months shift the macrophage populations in *Rb$^{+/-}$* mice. No significant changes in the relational proportions of the macrophage populations were found between *Rb$^{+/+}$* and *Rb$^{+/-}$* at the age of 2 months or 6 months (Figure 12). When collecting tissues, pituitaries were observed whether they showed signs of tumor development. Tumors or other morphological changes were not observed in the *Rb$^{+/-}$* animals at the age of 6 months. In conclusion, adenomas had not developed by the age of 6 months and the clear-symptoms phase occurs later in mice.
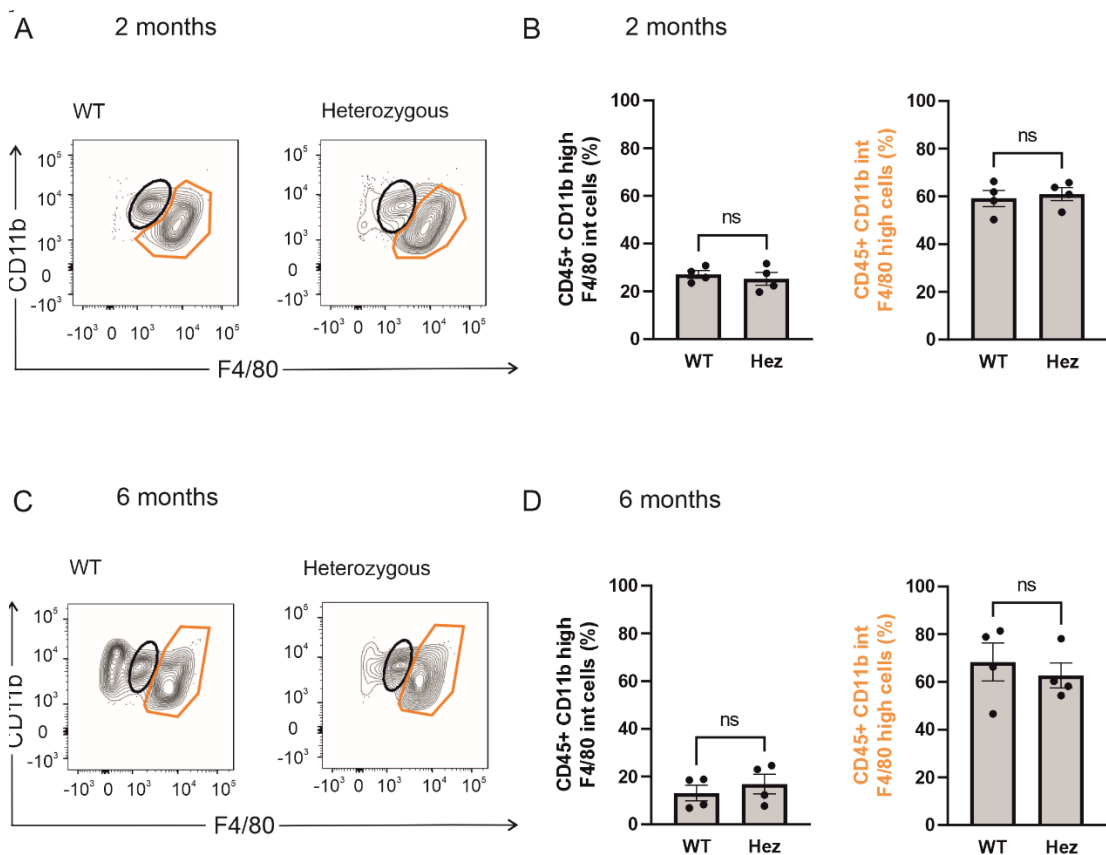

Figure 12. No significant changes were found in embryonic and bone marrow-derived macrophage populations in 2-months-old or 6-months-old retinoblastoma deficient male mice pituitaries. A & B presents relative proportions of CD11b^{high} F4/80^{int} and CD11b^{int} F4/80^{high} expressing populations between 2-months-old wild type (WT) *Rb$^{+/+}$* and heterozygous *Rb$^{+/-}$* mice. C & D presents relative proportions of 6-months-old wild type (WT) *Rb$^{+/+}$* and heterozygous *Rb$^{+/-}$* mice. CD11b^{int} F4/80^{high} embryonic-derived macrophage population is shown in orange and CD11b^{high} F4/80^{int} bone-marrow derived population is in black. Each dot represents one mouse and mean ± SEM are shown. ns = no significance, $p > 0.05$ (Mann-Whitney U Test).

3.4   Evaluation of retinoblastoma deficient mice pituitary gland histopathology

Histological staining was performed to evaluate the tumor progression and confirm the results from flow cytometric analyse of changing phenotypes of the pituitary resident macrophages in

the retinoblastoma deficient mice pituitary glands. Hematoxylin-eosin staining was used. In assumed clear-symptom phase, at 6-months-old, no clear alterations were observed in the histology between wild type $Rb^{+/+}$ and tumor-developing $Rb^{+/-}$ mice pituitary glands (Figure 13A). It was possible to collect only one 10-months-old Rb$^{+/-}$ mouse in the time window of this thesis. At 10 months of age, the heterozygous male mouse shown clear signs of adenoma in the dissection. The histological staining confirmed that tumor had developed in the mouse adenohypophysis. Clear alterations in the histology and structure of the pituitary gland were observed, including angiogenesis in the tumor (Figure 13B).
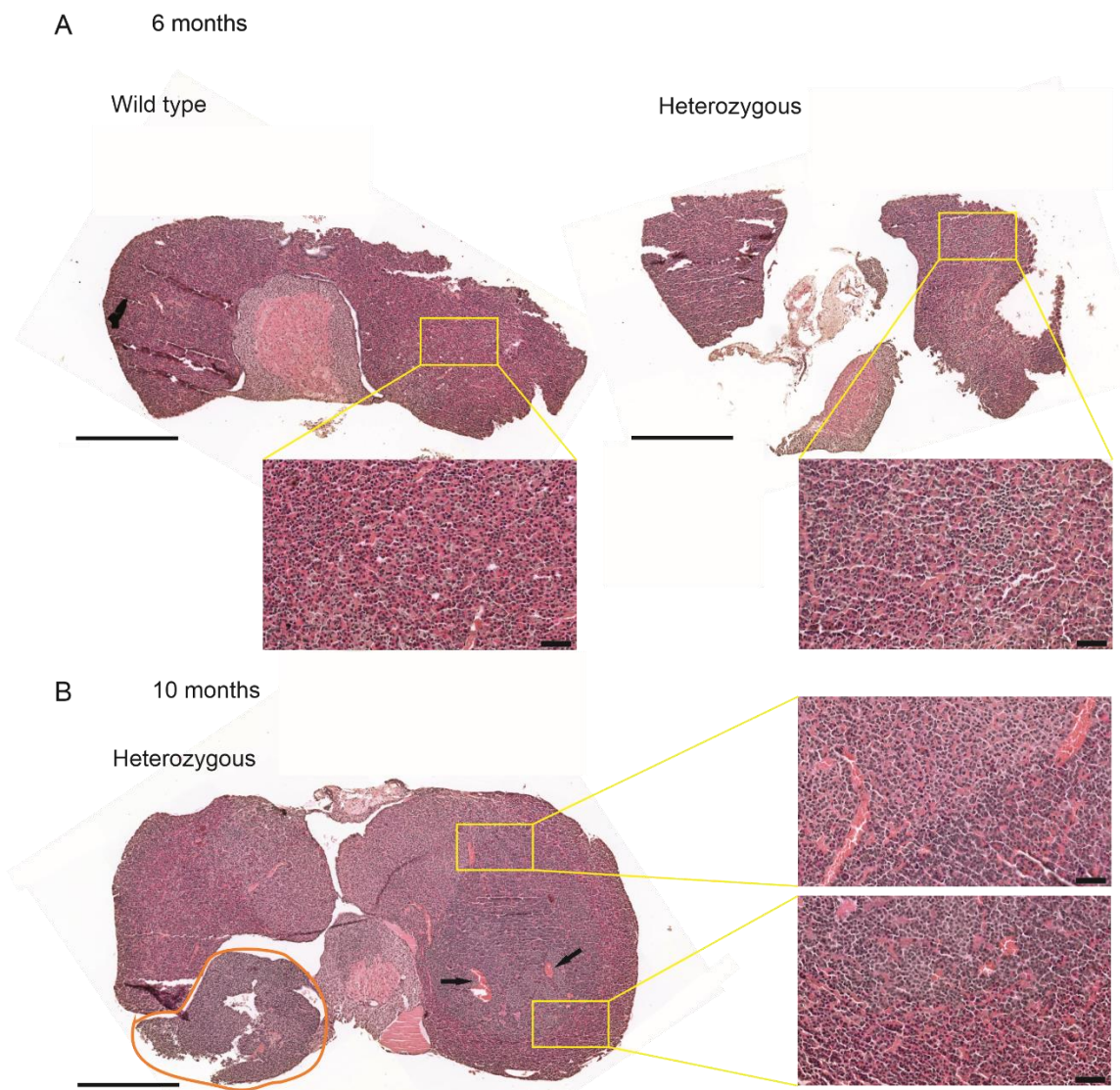
Figure 13. Histological staining of RB-mice pituitary gland at 6-months-old showed no alterations in heterozygous animal when at 10-months-old clear adenoma progression was observed. A. No clear signs of adenoma progression were observed in the histological staining of a wild type (Rb$^{+/+}$) and heterozygous (Rb$^{+/-}$) mouse pituitary glands. B. Clear histological alterations and tumor progression were observed at in 10-months-old heterozygous (Rb$^{+/-}$) mouse. Area surrounded in orange indicates excess growth of the adenohypophysis and arrows shows abnormal vasculature in the pituitary gland that can be due to angiogenesis in the tumor. Scale bars in the whole pituitary gland are 500 μm and in the closeups 10 μm.

4   Discussion

4.1   Immunohistochemical staining

In this master's thesis, immunohistochemical stainings were performed to determine the presence of macrophages in the mouse pituitary gland, and furthermore to study spatial relationships of macrophages and hormone-secreting endocrine cells. With whole-mount staining, we were able to show that macrophages have populated the prenatal pituitary gland and macrophages persist in the tissue during the postnatal development in mice. With F4/80 and MECA-32 double staining, pretentious and informative images were obtained. Analysis of the macrophage localisation and quantification would be possible with the double staining. F4/80 is a highly used macrophage marker in imaging and for example Hume and others (1984) were able to identify different macrophage populations in the mouse adenohypophysis and neurohypophysis based on the morphological features with the macrophage-specific antigen F4/80. This suggests that the observed changing morphology of maturing macrophages through the time series was valid.

Macrophages are involved in the endocrine function and development of the endocrine glands (Rehman et al. 2021). The knowledge of macrophage contribution to the development and function of the pituitary gland is still missing. The goal was to study macrophages in the relation to endocrine cells during mouse development and to shed light on their spatial relationships. Two different techniques of immunohistochemical staining were tested visualising endocrine cells in the mouse pituitary gland. From the five endocrine cell types that are present in the pituitary gland, LH- and GH-secreting cells were studied. The aim was to visualise LH-secreting gonadotropes and GH-secreting somatotropes with antibodies that interact with the secreted hormone. Unfortunately, the primary hormonal antibodies were found to be inoperable in the whole-mount staining. The result of the cell localisation of LH-secreting gonadotropes was unreliable due to the weak fluorescence signal and the possible partial staining that was limited in the edges of the rostral region of the pituitary. The study of the spatial relationships between macrophages and endocrine cells by using presented triple staining may falsify results if the staining of endocrine cells was incomplete.

Because of the poor signal or a complete malfunction of primary hormonal antibodies in the whole-mount staining, I decided to give a try to semi-squash staining and optimised collection and staining protocols for an adult mouse pituitary gland. With the semi-squash, a good signal of both, LH- and GH-secreting cells, was obtained using the same primary antibodies as in whole-mount. The results of the localisation of the studied endocrine cell types were in line with previous studies (le Tissier et al. 2012; Davis et al. 2011). The LH-secreting cells were located rostrally

but showed also mediolateral distribution and somatotropes were distributed throughout the gland. Even though the stainability was better in the semi-squash staining, the squashing alters the tissue structure. The localisation of cells can change and deform the spatial relationships of endocrine cells and macrophages. Also, if we wish to stain the vasculature of the gland to visualise tissue architecture, the squashing breaks the structure of the blood vessels and can alter the pituitary vascular network.

The whole-mount staining protocol could have been optimised for the hormonal antibodies. Harder fixation with 4% PFA could have been tried but it was known that the panendothelial antibody would not work if the PFA concentration was increased. Also, the antibody concentrations could have been increased and the primary antibodies could have been tested with different conjugates. The main reason, not to optimise the whole-mount staining further, was that the hormone antibodies did not work even in a single staining. However, the same antibodies worked well in semi-squash, suggesting that they just do not operate in whole-mount staining. The results suggest that the primary hormonal antibodies do not penetrate into the tissue in whole mount. Also, semi-squashed staining is more efficient, taking only two days. The triple whole-mount staining used in this thesis is a five-day process.

In whole-mount, handling of small tissues such as E17.5 and newborn pituitaries is problematic. In the clearing phase, it is not possible to keep the tissue in a planar level. Also, the tissue becomes transparent, making the clearing phase challenging. One cannot know where the tissue is located on the dish and there is a possibility of discarding it when removing BABB-solution. When samples were imaged, it was revealed that some of the samples had twisted from the other lateral wing. Luckily, the other later wing was always in a plane and suitable for imaging. The problem caused by the movement of samples during clearing, could be prevented by gluing the sample to the dish under a microscope before clearing.

The goal of the hormonal imaging was to study the relations of macrophages and endocrine cells during the development of the mouse pituitary gland. We used adult male mice to optimise the protocol because the gland is easier to handle based on its larger size. Also, older animals were used to ensure that the studied hormones are secreted. The semi-squash collection protocol needs further optimisation for early time points. At E17.5 and newborn, handling of the gland will be challenging because it is more of mucus than a solid gland. Also, its suitability for studying spatial relationships needs to be evaluated.

4.2 Origin of pituitary resident macrophages and the changing composition

The origin of pituitary resident macrophages is not known. Our results showed that in the prenatal and neonatal pituitary gland, two distinct tissue-resident macrophage populations were present. When combined expression of CD11b and F4/80 were studied with flow cytometry, two distinct populations were clearly distinguishable based on the signal intensities: CD11b^{int}F4/80^{high} and CD11b^{high}F4/80^{int}. Previous studies suggested that the CD11b^{int}F4/80^{high} expressing cells are derived from the yolk sac and the CD11b^{high}F4/80^{int} expressing cells are from the fetal liver (Ginhoux & Guilliams 2016). In these time points, the yolk sac-derived population was dominating in the pituitary gland.

To confirm that the CD11b^{int}F4/80^{high} expressing macrophage population originated from the yolk sac, cell-fate mapping studies were performed using reporter mice. With different reporter mouse models, the origin of tissue-resident macrophages in various tissues has been solved (Felix et al. 2021; Lokka et al. 2020; Jäppinen et al. 2019; Epelman et al. 2014). We crossed *Cx3cr1^{CreERT2}* males with *R26R-EYFP* females to generate tamoxifen-inducible reporter mice that express YFP signal in CX3CR1-expressing cells, such as macrophages. With the crossing, we were able to label the yolk sac-derived macrophages and follow their progeny when mice were induced with tamoxifen at E9.5.

With the cell-fate mapping study, it was proved that CD11b^{int}F4/80^{high} macrophages were derived from the yolk sac. When cells are labelled at E9.5, the yolk sac is the only structure that produces macrophages. The first wave of macrophages leaves from the yolk sac at E8.5 and populates brain and other tissues. It is followed by a second wave from the fetal liver at E12.5. The bone marrow activates during later development. This means that only yolk sac-derived macrophages will express the YFP-labelling in the E17.5 pituitary gland when labelled at E9.5. The result showed that all the labelled CD45+YFP+ cells were in the CD11b^{int}F4/80^{high} population which proves that the CD11b^{int}F4/80^{high} population is yolk sac-derived.

The tamoxifen labelling is never complete, wherein some of the cells appear as YFP negative. In Epelman and others' (2014) fate-mapping study of cardiac macrophage, around 30% of yolk sac-derived macrophages were labelled in adults when mice were induced at E8.5. The amount of tamoxifen that is given to a pregnant mouse is a balancing act between the desired labelling success and the successful pregnancy. Tamoxifen administration to pregnant mice during early pregnancy has been shown to disrupt pregnancy and perturb embryonic development (Ved et al. 2019). In the cell-fate mapping study, 1.5 mg tamoxifen was given with progesterone intra peritoneally. The amount of tamoxifen was sufficient to obtain YFP signal from the pituitary and

in the brain in the embryos (Supplement 2). Brains were used as a positive control. The brain houses yolk sac-derived macrophages in homeostasis without the contribution of bone marrow-derived macrophages to the macrophage pool (Ginhoux et al. 2016). Thus, the brain can be used as a positive control to confirm the labelling of the yolk sac-derived macrophages.

To show that the CD11b^{high}F4/80^{int} expressing population is derived from the fetal liver in prenatal and neonatal pituitaries in mice, we could use a mouse model that is lacking the liver-derived population. There is no cell-fate mapping model to track specifically fetal liver-derived macrophages. The tamoxifen induction to *Cx3cr1^{CreERT2};R26R-EYFP* during the second macrophage wave will lead to labelling of both the yolk sac and fetal liver macrophages. One fetal liver macrophage deficient mouse model is PLVAP deficient mice (*Plvap$^{-/-}$*) that have reduced numbers of fetal liver-derived macrophages in many tissues (Lokka et al. 2020; Jäppinen et al. 2019; Rantakari et al. 2015). Previous studies have shown a reduction of fetal liver macrophages in *Plvap$^{-/-}$* mice tissues when investigating the origin (Lokka et al. 2020; Jäppinen et al. 2019). Using *Plvap$^{-/-}$* mice, we could investigate is the CD11b^{high}F4/80^{int} population present in the mouse pituitary gland. If the population is missing or significantly reduced in the *Plvap$^{-/-}$* mouse pituitary, we could draw a conclusion that it is originated from the fetal liver. However, it is not possible to study macrophage composition in the *Plvap$^{-/-}$* mouse pituitary gland in early timepoints. The problem is caused by the small size of the pituitary gland at early timepoint and the high mortality of homozygous *Plvap$^{-/-}$* embryos. However, because the bone marrow starts to produce monocytes from hematopoietic stem cells in postnatal mice, we can conclude that bone marrow-derived macrophages cannot contribute to the prenatal and neonatal pituitary resident macrophage pool, thus, the unlabelled CD11b^{high}F4/80^{int} population is derived from the fetal liver.

The data suggested that in postnatal mice, two events changed the immunolandscape in the mouse pituitary gland. Firstly, a minor population shift occurred when fetal liver-derived macrophages changed their phenotype to CD11b^{int} F4/80^{high}. Secondly, the bone marrow-derived monocytes infiltrated into the pituitary gland and differentiated to pituitary resident macrophages. In 1-week-old mice, the populations shift had occurred and the CD11b^{high}F4/80^{int} expressing macrophage population was bone marrow-derived macrophages. To prove that the CD11b^{high}F4/80^{int} expressing macrophage population consists of bone marrow-derived macrophages, we could utilise a fate-mapping mouse model that allows the labelling of bone marrow-derived monocytes based on *Ms4a3* expression in granulo-monocyte progenitors (Liu et al. 2019). With Ms4a3^{Cre} and Rosa^{TdT} crossing, Liu and others (2019) were able to identify bone marrow-derived monocytes from tissue-resident macrophages. Also, mouse models that are deficient for bone marrow-derived monocytes could be used similarly as previously described. For example, CCR2

deficient mice (*Ccr2*$^{-/-}$) have significantly reduced monocyte number due to a lack of monocyte chemoattractant protein-1 that is involved in the migration of monocytes.

Study of the pituitary macrophages at early time points with flow cytometry was not effective. To get one sample, we needed to pool the whole litter at E17.5 embryos and from newborn to 2-weeks-old mice varying number of individuals. The quantity of animals in a pool in each time point was optimised. However, even after pooling, the experiments done with E17.5 and newborn mice had to be concatenated afterwards to get a sufficient amount of cells to analyse. The lower limit was set as at minimum of one thousand CD45+ cells. One thousand CD45+ cells ensure a suitable amount of cells remaining in the CD11b and F4/80 gating. Especially challenging was the newborn time point and the fact that only males were used. In one experiment, there were 4-6 newborn males born at a time. Newborn data consists of only three samples but these three samples required a total of 48 mice. The time point required a lot of repetitions because the number of cells obtained in one experiment was small. The small cell amount may be due to the weak aggregation of cells during the centrifugation, with a bigger proportion of cells being lost each time, compared to higher cell amounts. Also, the pituitary structure is different in E17.5 and newborn mice compared to the postnatal timepoints. The newborn mouse pituitary gland resembles more E17.5 pituitary gland than pituitary gland in a postnatal mouse. The protocol could be optimised for the early timepoints. Despite the problems caused by the small amount of starting material, flow cytometry is a powerful tool in the study of macrophage composition. The size of the pituitary gland limits the possibilities, for example studies with *Plvap*$^{-/-}$ mice embryos discussed before are not possible.

4.3 Functionality of pituitary macrophages in adenomas is unknown

Macrophages are contributors to tumorigenesis, but the studies of the macrophage composition and involvement in pituitary adenomas are lacking. CD11b+F4/80+ has been used to identify macrophages in tumors, but the invasive macrophage type has been identified using further markers such as CD68, CD206 and CD11c (Jin et al 2021; Zhang et al. 2021). Previous studies have shown that macrophages and monocytes are recruited into tumors attracted by soluble factors from the tumor microenvironment and hypoxic conditions (Zhang et al. 2021; Pollard et al. 2009). Principe and others (2020) were able to show that CD163+ macrophages showed an increase in addition to CD68+ cells in human gonadotroph tumors. Recent studies indicate that CD68+ macrophage number has significantly increased in pituitary adenomas (Lu et al. 2015). According to Lu and others (2015), all adenoma types show CD68+ macrophage infiltration. But there are noticeable differences in the infiltration between adenoma types in humans (Zhang et al. 2021).

To investigate the functionality of macrophages, the composition of macrophage subpopulations was studied in a cancer-developing mouse model, retinoblastoma deficient mice. The aim was to investigate, how does the tumor microenvironment change the composition of macrophage populations in the mouse pituitary gland. Studied time points were 2-months-old and 6-months-old mice. In both time points, wild type mouse (non-tumorous) was compared to tumor-developing heterozygous mouse. No significant differences in the relative amounts of $CD11b^{high}F4/80^{int}$ and $CD11b^{int}F4/80^{high}$ cells were found between the study groups. Tumor progression was evaluated in histological staining. No tumors were observed in the HE-staining of 6 months old RB-mice pituitary glands. Contrarily, a 10-months-old RB-mouse had developed a clear adenoma in the adenohypophysis and suggested that adenomas develop after 6 months in RB-mice.

For consistency and clarity, the composition of CD11b and F480 expressing macrophages was studied as a changing feature induced by the tumor microenvironment. The focus was on the relative amounts of $CD11b^{high}F4/80^{int}$ and $CD11b^{int}F4/80^{high}$ cells, not absolute cell amount per pituitary. However, a change in the relative expressions of the studied markers may indicate the phenotypic change from the anti-tumor phenotype into a TAM. With the flow-cytometric antibody-panel used in this thesis, CD163+ macrophages, CD206+ macrophages and monocytes (marker: Ly6C) can be further studied to evaluate the tumor progression and macrophage functionality (Supplement 1, table 4). However, it should be noted that some of the studies presented in this section have been conducted with human tissues and the suitability of the results should be assessed when assessing macrophage contribution based on the presented markers.

When starting the experiment trial, it was assumed that 6-months-old RB-mice would show a clear-symptom phase and the adenoma would have developed in the pituitary gland. However, that was not the case. The 6-months-old heterozygous mice did not show histological alterations in the pituitary gland. Also, in flow cytometric analyses, no significant difference in the CD11b+F480+ division was found between non-cancerous wild type mice and heterozygous tumor-developing genotype in either age points. In the time window of this thesis, it was possible for me to collect only one 10 month old heterozygous animal. At 10 months of age, clear tumor progression was present in the pituitary gland. Based on the results, the collection of the pituitary glands will be postponed that the animals are 9-10 months old and will be collected in the future.

Tumor microenvironment is a complex environment inducing multidimensional changes in the normal function of the immune system converting macrophages into TAMs. The studies discussed have shown specific macrophage phenotypes are enhanced in tumor microenvironments. In addition to changes in cell amounts, it has been shown that the tumor

environment suppresses T-cell activity and TAMs induce changes in other immune cells in a tumor, disrupting the immune responses (Farhood et al. 2019; Peng et al. 2017). The study of macrophage ontogeny will improve the understanding their function in homeostasis and activation. The ontogeny is valuable knowledge for creating optimal therapeutic strategies that target macrophages. In the active form of cancer immunotherapy, macrophages are promising targets. In immunotherapy, the tumor-inhibitory functions of macrophages can be induced or TAMs' tumor-promoting functions inhibited.

4.4   Summary

In this thesis, multiple methods were used to identify and study tissue-resident macrophages in the mouse pituitary gland. *In vivo* lineage tracking, flow cytometry and advanced imaging methods were combined with genetically modified mouse models were used.

The study demonstrated that macrophage populations are established prior the birth in the mouse pituitary gland. This was proved with both, imaging and flow cytometry. The results showed that the tissue-resident macrophage pool was derived from embryonic origins at E17.5 and newborn mice, indicating that yolk sac-derived macrophages dominate the immune landscape. With cell-fate mapping study with tamoxifen inducible reporter mice, it was proved that the dominating population is yolk sac-derived.

The results suggested that the composition of pituitary resident macrophage populations change in postnatal mice. At 1-week-old mouse pituitary, fetal liver-derived macrophages had changed their phenotype and bone marrow-derived macrophages contributed to the pool. Despite the infiltration of bone marrow-derived monocytes, embryonic-derived macrophages dominated in the adult pituitary gland in mice. The origin of bone marrow-derived macrophages is determined in further studies using mouse models suitable for tracking the bone marrow-derived monocytes.

In cancer, the role of macrophages is contradictory. Macrophages have been shown to have pro-tumoral function inducing the tumor progression, malignancy and increasing therapeutic resistance of cancer cells (Duan & Luo 2021). The tumor microenvironment is a major contributor to the generation of TAMs. In the tumor microenvironment certain phenotypes of macrophages are shown to increase, suggesting pro-tumor phenotypes (Zhang et al. 2021; Peng et al. 2017). In this thesis, the functionality of macrophages in pituitary adenomas was studied. The focus was on CD11b+F4/80+ macrophages and on the possible change in their relative amounts in tumor microenvironment. No significance change was found between the genotypes at 6 months. This

was confirmed with histological staining. As a result, we can conclude that retinoblastoma deficient mice had not developed adenoma at 6 months of age.

Immunotherapy in treating cancer is rapidly increasing. The mouse studies of macrophage ontogeny and phenotypic heterogeneity induced by signals from distinct tissue micro-environments have altered our understanding of these diverse and ingenious cells and led to the discovery of distinct subpopulations that reside in tissues. When developing novel therapeutic strategies human testing cannot be done. *In vivo* studies in animals provide valuable information, but the limitations when results are extrapolated to human needs to be evaluated.

Tissue-resident macrophages have a major role in maintaining homeostasis and normal function of tissues. Macrophages are involved in endocrine responses, for example generating, complex neuroimmunoendocrine integrity involved in the function of HPA. Pituitary gland operates the endocrine system interacting with the hypothalamus and peripheral target organs, creating multidimensional signaling pathways. The study of pituitary function is challenging because of its regulative function. The knowledge of the interaction between endocrine cells and macrophages during the development of the mouse pituitary gland remains still unknown.

Tissues house their own unique composition of tissue-resident macrophages in the steady state. Tissue-resident macrophage populations can maintain themselves independently, but monocyte infiltration can also contribute to the macrophage pool in the steady state. It was shown that macrophages populate the pituitary gland during the development of the mouse. In prenatal and neonatal mice, pituitary resident macrophages have originated from two ontogenically different sources, from the extraembryonic yolk sac and fetal liver. In postnatal mice, pituitary resident macrophages are derived from the three origins, including bone marrow-derived macrophages. Interestingly, the kinetic study, focusing on the relational proportions of the macrophage compartments, showed that the yolk sac-derived macrophages form the major population in the mouse pituitary gland through the development. This discovery is exceptional, and in this manner, the pituitary gland shows similar properties with the brain and differs from other endocrine glands. The brain houses only yolk sac-derived macrophages in steady state because the blood-brain barrier prevents circulating immune cells from entering into the postnatal brain. The location of the pituitary gland, under the brain, but still outside the blood-brain barrier, creates a unique immune environment. Even though the pituitary gland locates outside the blood-brain barrier, the infiltration of circulating monocytes was found to be a minor contributor in the macrophage pool. Our results provide interesting starting points to further investigate the pituitary resident macrophage function from an ontogenetic perspective in the future.

Acknowledgements

References

Aflorei ED & Korbonits M (2014). Epidemiology and etiopathogenesis of pituitary adenomas. *Journal of Neuro-Oncology* 117, 379–394.

Beishuizen A & Thijs LG (2004). The immunoneuroendocrine axis in critical illness: beneficial adaptation or neuroendocrine exhaustion? *Current Opinion in Critical Care* 10, 461-467.

Blériot C, Chakarov S, Ginhoux F (2020). Determinants of Resident Tissue Macrophage Identity and Function. *Immunity* 52, 957–970.

Budry L, Lafont C, el Yandouzi, T, Chauvet, N, Conéjero G, Drouin J, Mollard P (2011). Related pituitary celllineages develop into interdigitated 3D cell networks. *Proceedings of the National Academy of Sciences of the United States of America* 108, 12515–12520.

Cano DA, Soto-Moreno A, Cerro AL (2014). Genetically engineered mouse models of pituitary tumors. *Frontiers in Oncology* 4 JUL, 1–30.

Chanmee T, Ontong P, Konno K, Itano N (2014). Tumor-associated macrophages as major players in the tumor microenvironment. *Cancers* 6, 1670–1690.

Chen C, Hu Y, Lyu, L, Yin S, Yu Y, Jiang S, Zhou P (2021). Incidence, demographics, and survival of patients with primary pituitary tumors: a SEER database study in 2004–2016. *Scientific Reports* 11.

Cohen PE, Nishimura K, Zhu L, Pollard JW (1999). Macrophages: Important accessory cells for reproductive function. *Journal of Leukocyte Biology* 66, 765–772.

Davis SW, Mortensen AH, Camper SA (2011). Birthdating studies reshape models for pituitary gland cell specification. *Developmental Biology* 352, 215–227.

DeLeay M & Rieger A (2019). Flow Cytometry Handbook. *Bio-techne*. https://info.bio-techne.com/flowcytometry-handbook

Duan Z & Luo Y (2021). Targeting macrophages in cancer immunotherapy. *Signal Transduction and Targeted Therapy* 6.

Eguchi K & Manabe I (2013). Macrophages and islet inflammation in type 2 diabetes. *Diabetes, Obesity and Metabolism* 15, 152–158.

Epelman S, Lavine KJ, Beaudin AE, Sojka DK, Carrero JA, Calderon B, Brija T, Gautier EL, Ivanov S, Satpathy AT, Schilling JD, Schwendener R, Sergin I, Razani B, Forsberg EC, Yokoyama WM, Unanue ER, Colonna M, Randolph GJ, Mann DL (2014). Embryonic and adult-derived resident cardiac macrophages are maintained through distinct mechanisms at steady state and during inflammation. *Immunity* 40, 91–104.

Farhood B, Najafi M, Mortezaee K (2019). CD8+ cytotoxic T lymphocytes in cancer immunotherapy: A review. *Journal of Cellular Physiology* 234, 8509–8521.

Félix I, Jokela H, Karhula J, Kotaja N, Savontaus E, Salmi M, Rantakari P (2021). Single-Cell Proteomics Reveals the Defined Heterogeneity of Resident Macrophages in White Adipose Tissue. *Frontiers in Immunology* 12.

Fujiyama S, Nakahashi-Oda C, Abe F, Wang Y, Sato K, Shibuya A (2018). Identification and isolation of splenic tissue-resident macrophage sub-populations by flow cytometry. *International Immunology* 31, 51–56.

Geutskens SB, Otonkoski T, Pulkkinen M-A, Drexhage HA, Leenen PJM (2005). Macrophages in the murine pancreas and their involvement in fetal endocrine development in vitro. *Journal of Leukocyte Biology* 78, 845–852.

Ginhoux F & Guilliams M (2016). Tissue-Resident Macrophage Ontogeny and Homeostasis. *Immunity* 44, 439–449.

Ginhoux F, Schultze JL, Murray PJ, Ochando J, Biswas SK (2016). New insights into the multidimesionalconcept of macrophage ontogeny, activation and function. *Nature Immunology* 17, 34–40.

Hoeffel G, Chen J, Lavin Y, Low D, Almeida FF, See P, Beaudin AE, Lum J, Low I, Forsberg EC, Poidinger M, Zolezzi F, Larbi A, Ng LG, Chan JKY, Greter M, Becher B, Samokhvalov IM, Merad M, Ginhoux F (2015). C-Myb+ Erythro-Myeloid Progenitor-Derived Fetal Monocytes Give Rise to Adult Tissue-Resident Macrophages. *Immunity* 42, 665–678.

Hoeffel G & Ginhoux F (2018). Fetal monocytes and the origins of tissue-resident macrophages. *Cellular Immunology* 330, 5–15.

Hume DA, Halpintt D, Charltont H, Gordon S (1984). The mononuclear phagocyte system of the mouse defined by immunohistochemical localization of antigen F4/80: Macrophages of endocrine organs (pituitary/adrenal cortex/ccorpus luteum/testis). *The Proceedings of the National Academy of Sciences USA* 81.

Jacks T, Fazeli, A, Schmitt EM, Bronsont RT, Goodell MA, Weinberg RA (1992). Effects of an Rb mutation in the mouse. *Nature* 359, 295–300.

Jenkins SJ & Allen JE (2021). The expanding world of tissue-resident macrophages. European *Journal of Immunology* 51, 1882–1896.

Jin J, Lin J, Xu A, Lou J, Qian C, Li X, Wang Y, Yu W, Tao H (2021). CCL2: An Important Mediator Between Tumor Cells and Host Cells in Tumor Microenvironment. *Frontiers in Oncology* 11.

Jokela H, Lokka E, Kiviranta M, Tyystjärvi S, Gerke H, Elima K, Salmi M, Rantakari P (2020). Fetal-derived macrophages persist and sequentially mature in ovaries after birth in mice. *European Journal of Immunology* 50, 1500–1514.

Jurberg AD, Cotta-de-Almeida V, Temerozo JR, Savino W, Bou-Habib DC, Riederer I (2018). Neuroendocrine control of macrophage development and function. *Frontiers in Immunology* 9.

Jäppinen N, Félix, I, Lokka E, Tyystjärvi S, Pynttäri A, Lahtela T, Gerke H, Elima K, Rantakari P, Salmi M (2019). Fetal-derived macrophages dominate in adult mammary glands. *Nature Communications* 10.

Kim H, Kim M, Im S-K, Fang S (2018). Mouse Cre-LoxP system: general principles to determine tissue-specific roles of target genes. *Laboratory Animal Research* 34, 147.

Larkin S & Ansorge O (2017). Development And Microscopic Anatomy Of The Pituitary Gland. *Endotext*. <https://www.ncbi.nlm.nih.gov/sites/books/NBK425703/> [Visited: 10.2.2022].

le Tissier PR, Hodson DJ, Lafont C, Fontanaud P, Schaeffer M, Mollard P (2012). Anterior pituitary cell networks. *Frontiers in Neuroendocrinology* 33, 252–266.

Liu Z, Gu Y, Chakarov S, Bleriot C, Kwok I, Chen X, Shin A, Huang W, Dress RJ, Dutertre C A, Schlitzer A, Chen J, Ng LG, Wang H, Liu Z, Su B, Ginhoux F (2019). Fate Mapping via Ms4a3-Expression History Traces Monocyte-Derived Cells. *Cell* 178, 1509-1525.

Lokka E, Lintukorpi L, Cisneros-Montalvo S, Mäkelä JA, Tyystjärvi S, Ojasalo V, Gerke H, Toppari J, Rantakari P, Salmi M (2020). Generation, localization and functions of macrophages during the development of testis. *Nature Communications* 11.

Lu JQ, Adam B, Jack AS, Lam A, Broad RW, Chik CL (2015). Immune Cell Infiltrates in Pituitary Adenomas: More Macrophages in Larger Adenomas and More T Cells in Growth Hormone Adenomas. *Endocrine Pathology* 26, 263–272.

Mass E (2018). Delineating the origins, developmental programs and homeostatic functions of tissue-resident macrophages. *International Immunology* 30, 493–501.

Metzger D & Chambon P (2001). Site- and time-specific gene targeting in the mouse. *Methods* 24, 71–80.

Molitch ME (2017). Diagnosis and treatment of pituitary adenomas: A review. *Journal of the American Medical Association* 317, 516–524.

Munro DAD & Hughes J (2017). The origins and functions of tissue-resident macrophages in kidney development. *Frontiers in Physiology* 8.

Ooi GT, Tawadros N, Escalona RM (2004). Pituitary cell lines and their endocrine applications. *Molecular and Cellular Endocrinology* 2281–21.

Peng LS, Zhang JY, Teng YS, Zhao YL, Wang TT, Mao FY, Lv YP, Cheng P, Li WH, Chen N, Duan M, Chen W, Guo G, Zou QM, Zhuang Y (2017). Tumor-associated monocytes/macrophages impair NK-cell function via TGFβ1 in human gastric cancer. *Cancer Immunology Research* 5, 248–256.

Pollard JW (2009). Trophic macrophages in development and disease. *Nature Reviews Immunology* 9, 259–270.

Pollard JW, Dominguez MG, Mocci S, Cohen PE, Stanley ER (1997). Effect of the Colony-Stimulating Factor-1 Null Mutation, Osteopetrotic (csfmoP), on the Distribution of Macrophages in the Male Mouse Reproductive Tract'. *BIOLOGY OF REPRODUCTION* 56.

Principe M, Chanal M, Ilie MD, Ziverec A, Vasiljevic A, Jouanneau E, Hennino A, Raverot G, Bertolino P (2020). Immune Landscape of PituitaryTumors Reveals Association between Macrophages and Gonadotroph Tumor Invasion. *Journal of Clinical Endocrinology and Metabolism* 105.

Rantakari P, Auvinen K, Jäppinen N, Kapraali M, Valtonen J, Karikoski M, Gerke H, Iftakhar-E-Khuda I, Keuschnigg J, Umemoto E, Tohya K, Miyasaka M, Elima K, Jalkanen S, Salmi M (2015). The endothelial protein PLVAP in lymphatics controls the entry of lymphocytes and antigens into lymph nodes. *Nature Immunology* 16, 386–396.

Rao R & Honavar SG (2017). Retinoblastoma. *Indian Journal of Pediatrics* 84, 937–944.

Rehman A, Pacher P, Haskó G (2021). Role of Macrophages in the Endocrine System. *Trends in Endocrinology and Metabolism* 32, 238–256.

Shaw TN, Houston SA, Wemyss K, Bridgeman HM, Barbera TA, Zangerle-Murray T, Strangward P, Ridley AJL, Wang P, Tamoutounour S, Allen JE, Konkel JE, Grainger JR (2018). Tissue-resident macrophages in the intestine are long lived and defined by Tim-4 and CD4 expression. *Journal of Experimental Medicine* 215, 1507–1518.

Schulz C, Gomez Perdiguero E, Chorro L, Szabo-Rogers H, Cagnard N, Kierdorf K, Prinz M, Wu B, Jacobsen SE, Pollard JW, Frampton J, Liu KJ, Geissmann F (2012). A lineage of myeloid cells independent of Myb andhematopoietic stem cells. *Science* 6, 86-90.

Sheng JA, Bales NJ, Myers SA, Bautista AI, Roueinfar M, Hale TM, Handa RJ (2021). The Hypothalamic-Pituitary-Adrenal Axis: Development, Programming Actions of Hormones, and Maternal-Fetal Interactions. *Frontiers in Behavioral Neuroscience* 14.

Utz SG, See P, Mildenberger W, Thion MS, Silvin A, Lutz M, Ingelfinger F, Rayan NA, Lelios I, Buttgereit A, Asano K, Prabhakar S, Garel S, Becher B, Ginhoux F, Greter M (2020). Early Fate Defines Microglia and Non-parenchymal Brain Macrophage Development. *Cell* 181, 557-573.

Ved N, Curran A, Ashcroft FM, Sparrow DB (2019). Tamoxifen administration in pregnant mice can be deleterious to both mother and embryo. *Laboratory Animals* 53, 630–633.

Williams CB, Yeh ES, Soloff AC (2016). Tumor-associated macrophages: Unwitting accomplices in breast cancer malignancy. *Breast Cancer* 2.

Yang Q, Wang Y, Pei G, Deng X, Jiang H, Wu J, Zhou C, Guo Y, Yao Y, Zeng R, Xu G (2019). Bone marrow-derived Ly6C− macrophages promote ischemia-induced chronic kidney disease. *Cell Death and Disease* 10.

Yona S, Kim KW, Wolf Y, Mildner A, Varol D, Breker M, Strauss-Ayali D, Viukov S, Guilliams M, Misharin A, Hume DA, Perlman, H, Malissen B, Zelzer E, Jung S (2013). Fate Mapping Reveals Origins and Dynamics of Monocytes and Tissue Macrophages under Homeostasis. *Immunity* 38, 79–91.

Zhang A, Xu Y, Xu H, Ren J, Meng T, Ni Y, Zhu Q, Zhang WB, Pan YB, Jin J, Bi Y, Wu ZB, Lin S, Lou M (2021). Lactate-induced M2 polarization of tumor-associated macrophages promotes the invasion of pituitary adenoma by secreting CCL17. *Theranostics* 11, 3839–3852.

Zhu X, Lin C, Prefontaine GG, Tollkuhn J, Rosenfeld MG (2005). Genetic control of pituitary development and hypopituitarism. *Current Opinion in Genetics & Development* 15, 332–340.

Supplements

Supplement 1. Antibody panels and solutions for flow cytometry:

Table 1. Antibody panel for reporter mice (*Cx3cr1^{CreERT2} x Rosa26-EYFP)* pituitary

Antigen	Fluorochrome	Reactivity	Manufacturer & catalog number	Dilution
CD45	PerCP-5.5	Rat anti-mouse	BD Biosciences, 550994	1:200
CD11b	BV786	Rat anti-mouse	BD Biosciences 740861	1:400
F4/80	BV510	Rat anti-mouse	BioLegend, 123135	1:100
CD64	PE	Mouse anti-mouse	Biolegend, 139304	1:200
MHCII	BV711	Rat anti-mouse	BD Biosciences, 563414	1:200
CD206	BV650	Rat anti-mouse	BioLegend, 141723	1:200
CD163	A647	Rat anti-mouse	Self-conjugated	1:200
CD43	Pe-Cy7	Rat anti-Mouse	BD Bioscinces, 562866	1:400
Ly6C	BV421	Rat anti-Mouse	BD Biosciences, 562727	1:200

Table 2. Antibody panel for E17.5 and newborn C57BL/6NRj mice

Antigen	Fluorochrome	Reactivity	Manufacturer & catalog number	Dilution
CD45	PerCP-5,5	Rat anti-mouse	BD Biosciences, 550994	1:200
CD11b	BV786	Rat anti-mouse	BD Biosciences 740861	1:400
F4/80	A488	Rat anti-mouse	eBioscience, 53-4801-82	1:200
CD64	PE	Mouse anti-mouse	Biolegend, 139304	1:200
MHCII	BV711	Rat anti-mouse	BD Biosciences, 563414	1:200
CD206	BV650	Rat anti-mouse	BioLegend, 141723	1:200
CD163	A647	Rat anti-mouse	Self-conjugated	1:200
SiglecH	BV510	Rat anti-mouse	BD Biosciences, 747674	1:200
CD43	Pe-Cy7	Rat anti-Mouse	BD Biosciences, 562866	1:400
Ly6C	BV421	Rat anti-Mouse	BD Biosciences, 562727	1:200

Table 3. Antibody panel for 1-week to 8weeks-old C57BL/6NRj mice

Antigen	Fluorochrome	Reactivity	Manufacturer & catalog number	Dilution
CD45	PerCP-5,5	Rat anti-mouse	BD Biosciences, 550994	1:200
CD11b	BV786	Rat anti-mouse	BD Biosciences 740861	1:400
F4/80	A488	Rat anti-mouse	eBioscience, 53-4801-82	1:200
CD64	PE	Mouse anti-mouse	Biolegend, 139304	1:200
MHCII	BV711	Rat anti-mouse	BD Biosciences, 563414	1:200
CD206	BV650	Rat anti-mouse	BioLegend, 141723	1:200
Ly6C	A647	Rat anti-mouse	Elabscience, E-AB-F1121M	1:200
SiglecH	BV510	Rat anti-mouse	BD Biosciences, 747674	1:200
CD43	Pe-Cy7	Rat anti-mouse	BD Biosciences, 562866	1:400
CD3e	BV421	Rat anti-mouse	BD Biosciences, 562600	1:200
CD44	PE-CF594	Rat anti-mouse	BD Biosciences, 562464	1:200

Table 4. Antibody panel for retinoblastoma deficient mice

Antigen	Fluorochrome	Reactivity	Manufacturer & catalog number	Dilution
CD45	PerCP-5,5	Rat anti-mouse	BD Biosciences, 550994	1:200
CD11b	BV510	Rat anti-mouse	BioLegend, 101263	1:200
F4/80	A488	Rat anti-mouse	eBioscience, 53-4801-82	1:200
CD64	BV786	Rat anti-mouse	BD Biosciences, 741024	1:200
MHCII	BV711	Rat anti-mouse	BD Biosciences, 563414	1:200
CD206	BV650	Rat anti-mouse	BioLegend, 141723	1:200
CD163	A647	Rat anti-mouse	Self-conjugated	1:200
CD115	Pe-Cy7	Rat anti-Mouse	eBioscience, 25-1152-80	1:400
Ly6C	BV421	Rat anti-Mouse	BD Biosciences, 562727	1:200
Lyve1	PE	Rat anti-mouse	R&D Systems, FAB2125P	1:200

Flow cytometry staining solutions

EPICS PBS

1:10 10x PBS (BP399-4, Thermo Fisher Scientific) in Milli-Q water

EPICS I

40 ml EPICS PBS

0.8 ml fetal calf serum (Biowest)

0,04 ml 4% NaN$_3$

EPICS FIX

20 ml EPICS PBS

0,54 ml 37 % formaldehyde (1.04002, Merck)

Supplement 2. Solutions for whole-mount staining

PBS

1:10 10x PBS (BP399-1, Thermo Fisher Scientific) in MilliQ water

Blocking solution

1% normal goat serum (005-000-121, Jackson ImmunoResearch)

0.5 % fetal calf serum (Biowest)

1 % bovine serum albumin (P6154, Biowest)

0.4% Triton X-100 (T8787, Sigma)

in PBS

Washing solution

1 % bovine serum albumin (P6154, Biowest)

0.4% Triton X-100 (T8787, Sigma)

in PBS

Supplement 3. Tamoxifen labelling of yolk sac-derived microglia in the brain

Brain was use as a positive control in the cell-fate mapping study conducted in E17.5 *Cx3cr1^{CreERT2}* x *Rosa26-EYFP* mice. Microglia are yolk sac-derived and they should express YFP if the labelling has been successful. Side-scattering (SSC) and forward scattering (FSC) were used to eliminate dead cells and cell aggregates. Live cells were gated based LIVE/DEAD-marker that stains dead cells and live cells remain negative. CD45+ cells were gated as leukocytes from live cells. Microglia was gated as CD45+CD11b+. From microglia YFP+ cells were gated to confirm the labelling success of yolk sac-derived macrophages (Figure 1).
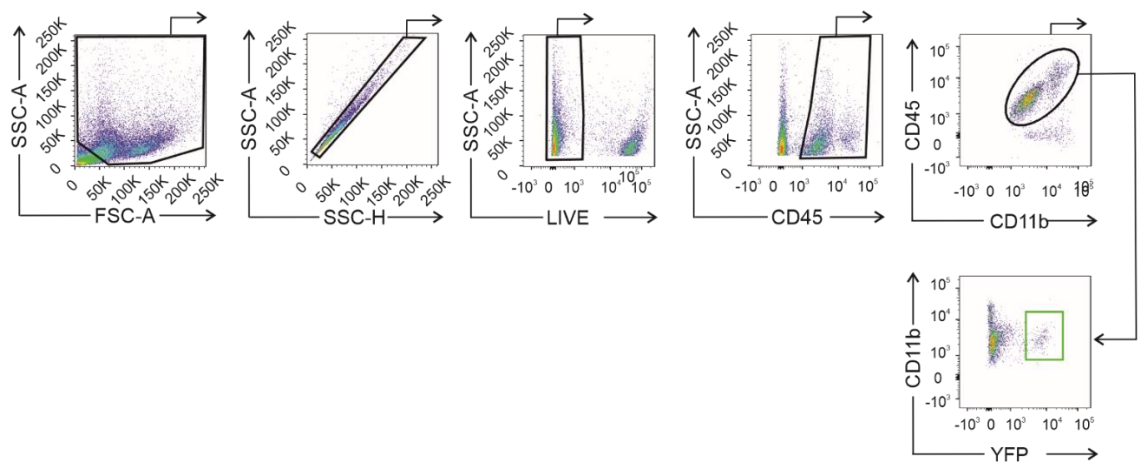

Figure 1. Gating strategy of at E9.5 tamoxifen labelled brain microglia in E17.5 *Cx3cr1^{CreERT2}* x *Rosa26-EYFP* offspring. The flow cytometric analysis of labelled YFP+ cells confirmed the labelling success in the cell-fate mapping study of yolk sac-derived macrophages.